

4-4-6 Description of polished sections of ore

Polished sections of ore, mainly of massive sulphide ores, were examined under the microscope. The results are shown in Table II-4-3. The following are descriptions of the main constituent minerals, such as pyrite, chalcopyrite, hematite and magnetite. Photographs of these minerals under the microscope are shown in Appendix 5.

(1) Pyrite

Based on their occurrences, pyrites observed in massive sulphide ores are divided into two groups:

(a) First group of the pyrites consists of fine to coarse grained euhedral and subhedral pyrite crystals as shown in Photo.1(G5-147.80), and are fractured in many cases. The fractures and spaces between small pyrite fragments are filled by chalcopyrite and gangue minerals. Depending on the intensity of fracturing, different characteristics can be observed in this group of pyrites, such as, pyrite crystals with only fine network-like fractures(Photo.2; G11-163.00), pyrite crystals with fine stockwork chalcopyrite found in pyrite crystal(Photo.3; G14-132.20) and small pyrite fragments contained in fine grained matrix of chalcopyrite(Photo.4; G15-189.00). This group of pyrites is accompanied by only a small numbers of vesicles and showing, in general, a smooth polished surface. Spaces between the crystals are filled by chalcopyrite, gangue minerals and either fine grained pyrite or very fine grained pyrite forming colloform texture(Photo.5, G14-150.00).

(b) The second group includes a colloform textured aggregate of very fine grained anhedral pyrites, an irregular shaped and vesicular aggregate of fine to very fine grained pyrites and a fine grained single euhedral pyrite crystals as well. The aggregate of colloform textured pyrites shows a very fine grained with either globular or botryoidal texture(Photo.6; G3-136.90, Photo.7; G3-134.50, Photo 8; G5-147.80), and a chalcopyrite and gangue minerals are observed in the core or between crystals. Since the aggregate of colloform texture and irregular shaped are filling the spaces between medium to coarse grained pyrite crystals(Photo.9; G5-147.80), these were formed evidently after the formation of first group of pyrite. Colloform texture of sulphide minerals can be observed in the ores which crystalized after precipitation of sulphide gel formed by the rapid cooling of hydrothermal solution in a open space.

(2) Chalcopyrite

All of chalcopyrite crystals are unhedral. Most of them are filling spaces either between pyrite crystals or fractures developed in pyrite crystals, and some are filling either the spaces between very

fine grained pyrite crystals of colloform textured aggregate or the core of aggregate. Comparing with pyrite, chalcopyrites have less numbers of fractures and vesicles.

(3) Hematite and magnetite

Samples of G11-163.00 and G17-222.70 contain very small scale and flaky hematites which show a reddish internal reflection in quartz crystals under microscope (Photo.11; G11-163.00). In the sample of G11-163.00, lath-shaped magnetites and hematites are observed in gangue minerals as shown in Photo.12. Since magnetite is presented in hexagonal systems and tends to form granular crystals in nature, it is considered that these lath-shaped magnetites were formed secondarily from hematite by a reduction process and are showing the pseudomorphs of hematites. This fact suggests the idea that the condition of oxidation and reduction changed during the hydrothermal process.

4-5 Discussion

The results of drilling surveys are discussed individually for each area as follows:

4-5-1 Ghuzayn area

Two massive sulphide ore bodies were discovered during this survey, i.e., the Northern body intersected by the boreholes of MJOB-G3 and G13 and the Western body intersected by the boreholes MJOB-G5, G14, G15, G16 and G17. Table II-4-5 presents a summary of these results, including their scales and assays.

Geologic cross sections in bore hole sites located on the Northern and Western bodies are shown in Figs. II-4-5 and II-4-6, while the TDIP pseudo-sections containing the crossing boreholes are illustrated in Figs. II-4-7 and II-4-8. The distribution of the boundaries between Lower extrusive 1 and Lower extrusive 2 and the massive sulphide ore bodies detected in the above holes give more clarifications on the general geologic structure in Ghuzayn area. According to Figs. II-4-5 and II-4-6, the volcanic rocks and massive orebodies in this area, trend northeast to southwest and dips by 15 to 30° northwest.

Stockwork zone is known to accompany the Cyprus-type massive sulphide deposits as shown in Fig. II-4-9 of the schematic model of Daris and Rakah deposits. In Ghuzayn area, this stockwork ores are found in MJOB-G3 at Northern body and MJOB-G14 at Western body. Since a stockwork ore could be formed in and around a pass of hydrothermal solution which produced massive sulphide ore bodies, the main fault where a hydrothermal solution passed mainly through could be found nearby each of the borehole G3 and G14. The results of drilling and TEM surveys on Western body support

Table II-4-5 Summary of results on drilling survey in Ghuzayn area

Ore Body Name	Bore Hole NO.	Type of Ore	Depth (m)		Thickness (m)	Average Grade	
			from	to		Cu%	Zn(%)
Ghuzayn Northern Body	MJOB-G3	stockwork(upper)	115.15	133.00	17.85	0.22	0.01
		massive sulphide	133.45	138.60	5.15	4.85	0.04
		massive sulphide	140.00	142.80	2.80	3.77	0.06
		stockwork(lower)	142.80	166.65	23.85	0.40	0.11
		stockwork(lower)	167.15	179.90	12.75	0.59	0.03
		stockwork(lower)	185.35	233.50	48.15	0.27	0.02
		stockwork(lower)	246.10	247.25	1.15	0.30	0.17
		stockwork(lower)	279.50	288.20	8.70	0.15	2.66
		MJOB-G13	massive sulphide	152.80	154.40	1.60	0.17
Ghuzayn Western Body	MJOB-G5	stockwork	134.00	136.90	2.90	0.33	0.01
		massive sulphide	136.90	170.60	33.70	1.47	0.04
	MJOB-G14	massive sulphide	119.80	164.75	37.10	1.88	0.04
		stockwork	164.75	171.50	6.75	2.74	0.44
		stockwork	171.50	230.50	59.00	0.37	0.32
	MJOB-G15	(metaliferous sediment)	178.85	179.20	0.35	2.10	0.01
		massive sulphide	179.20	212.30	29.90	1.55	0.05
	MJOB-G16	stockwork	186.30	186.90	0.60	0.14	0.04
		massive sulphide	186.90	189.40	2.50	1.63	0.05
	MJOB-G17	massive sulphide	215.90	222.80	6.90	1.17	0.05

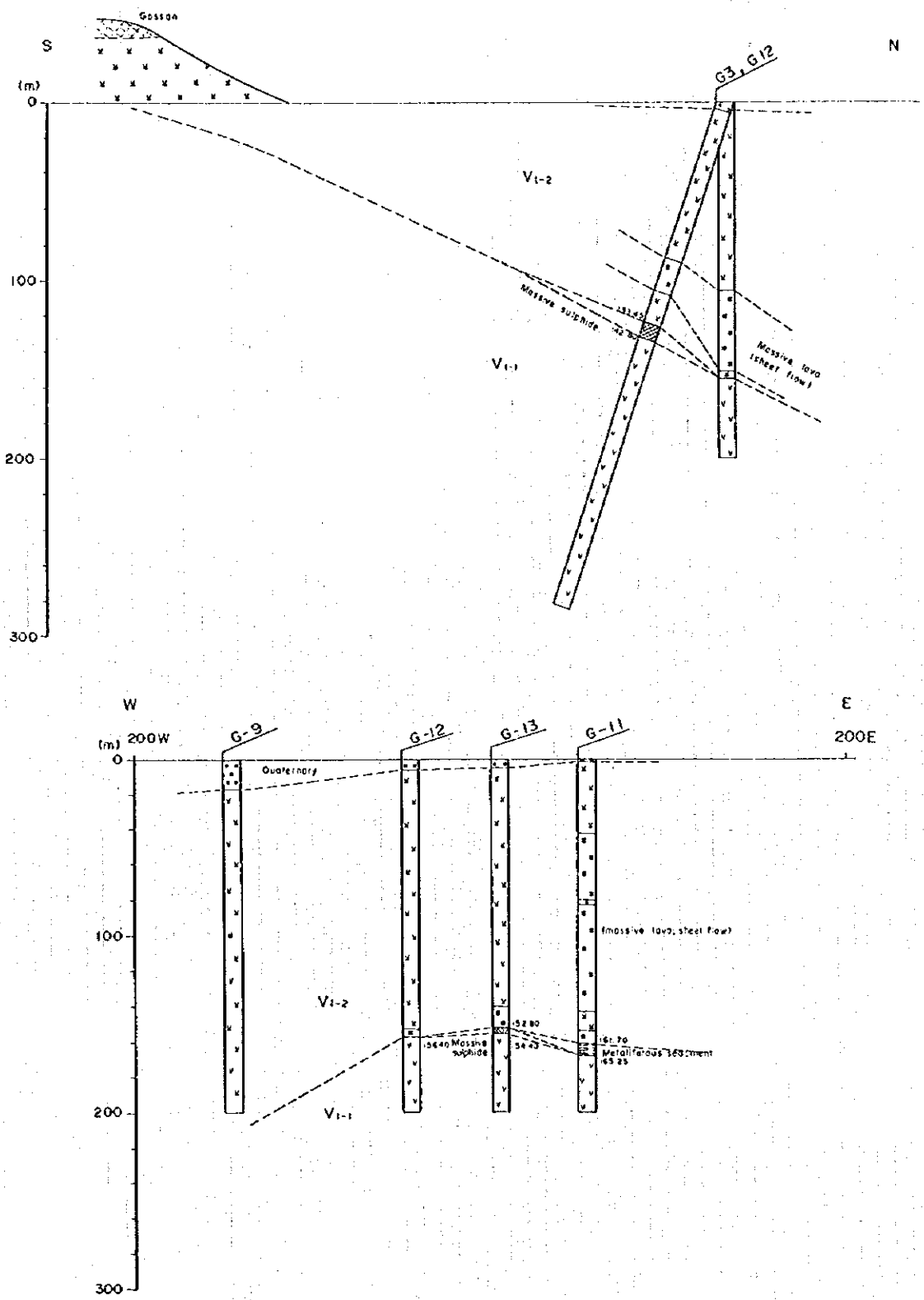


Fig.II-4-5 Cross section of borehole site in the northern body of Ghuzayn deposit

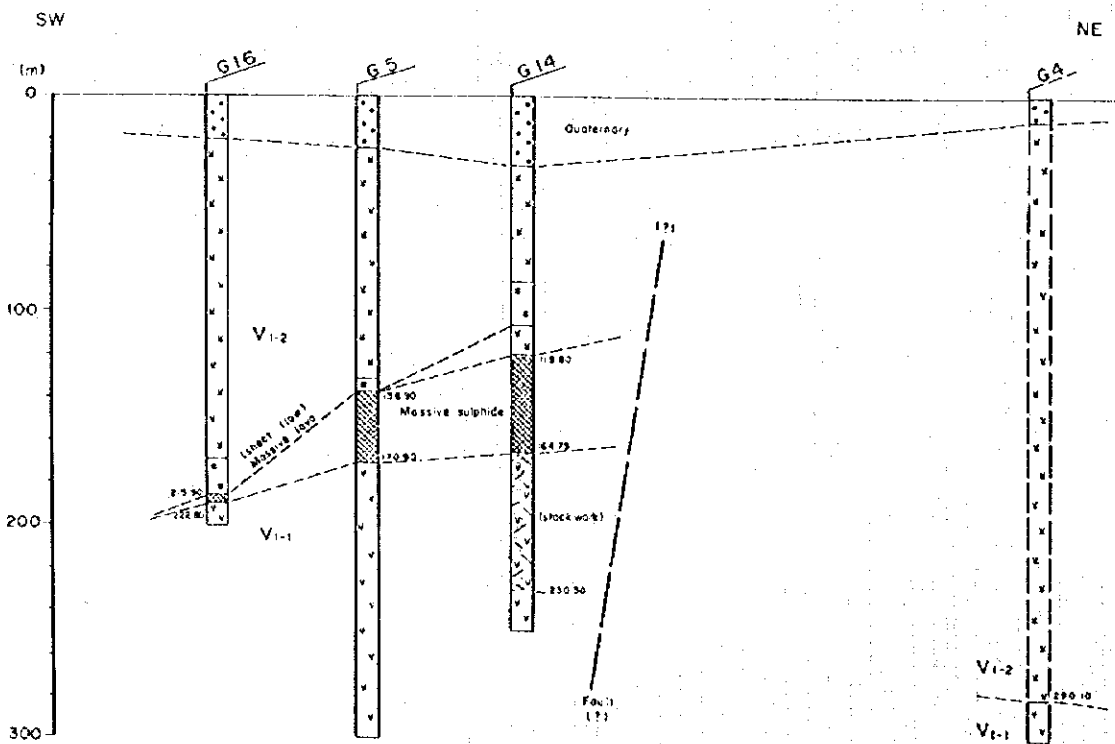
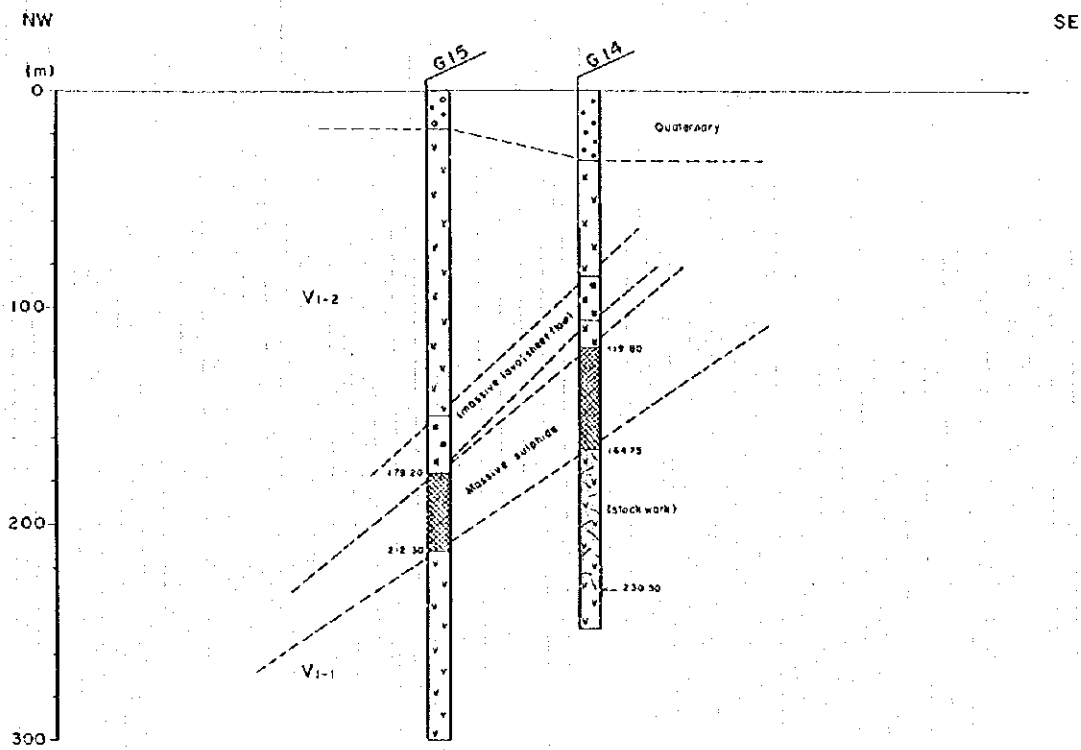


Fig.II-4-6 Cross section of borehole site in the western body of Ghuzayn deposit

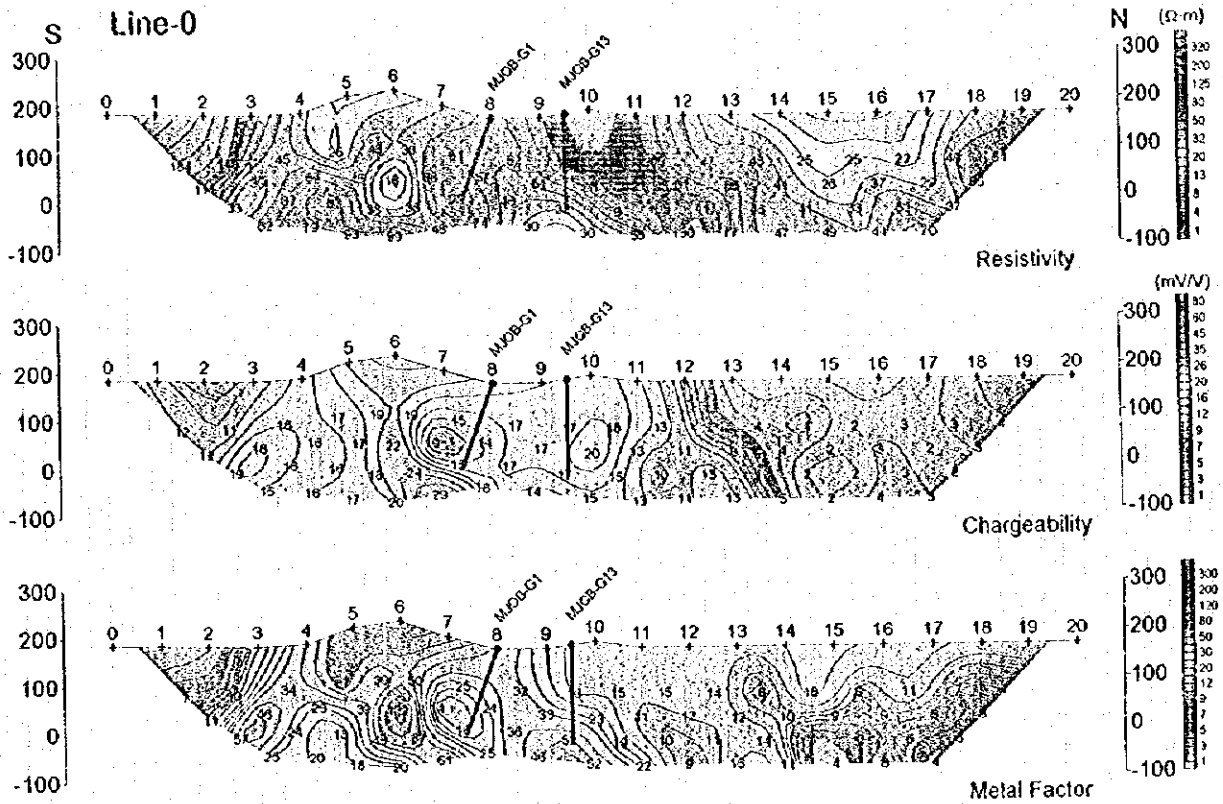


Fig.II-4-7 IP pseudo-section around northern body of Ghuzayn deposit

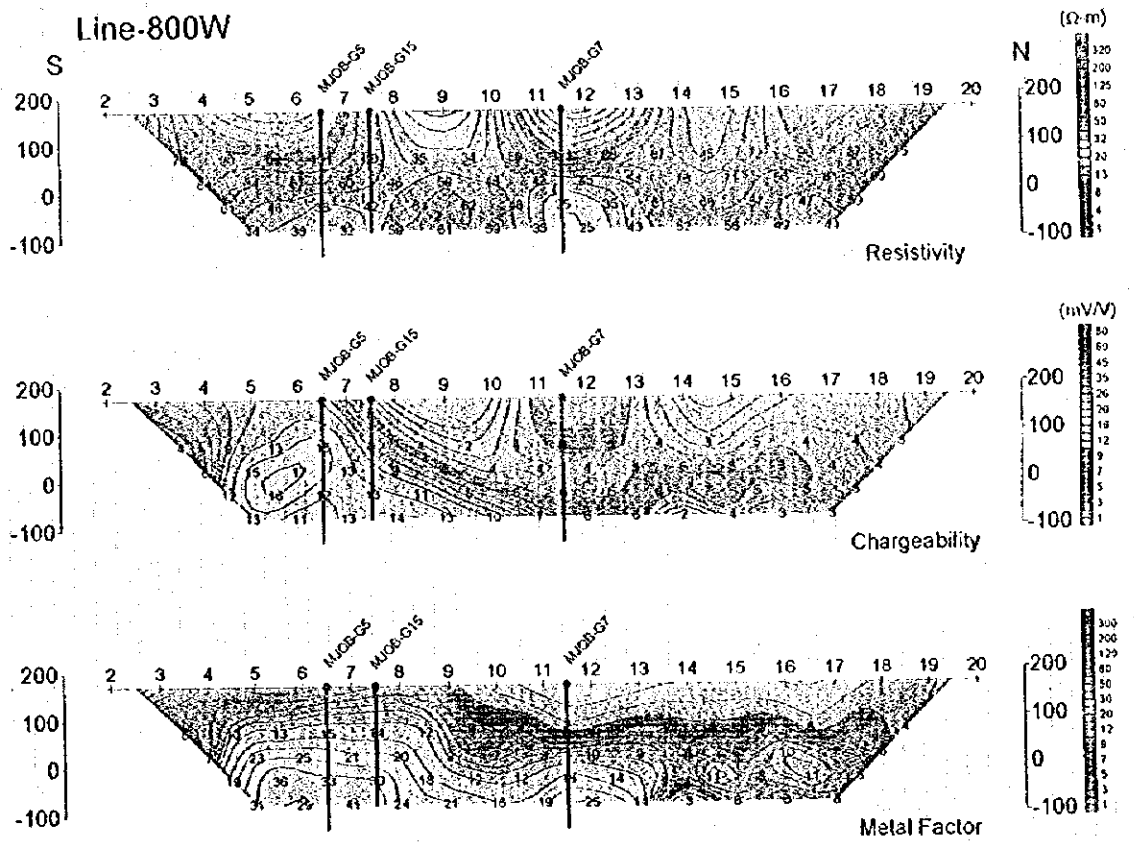
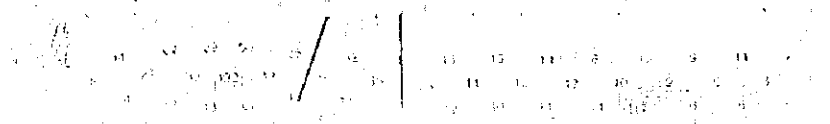
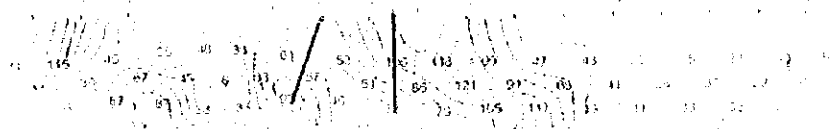


Fig.II-4-8 IP pseudo-section around western body of Ghuzayn deposit

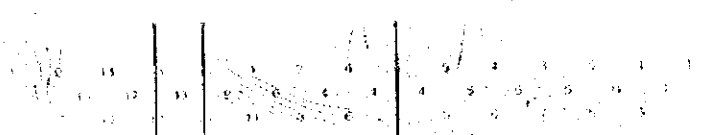
S Line 0

1000
900
800
700
600
500
400
300
200
100
0

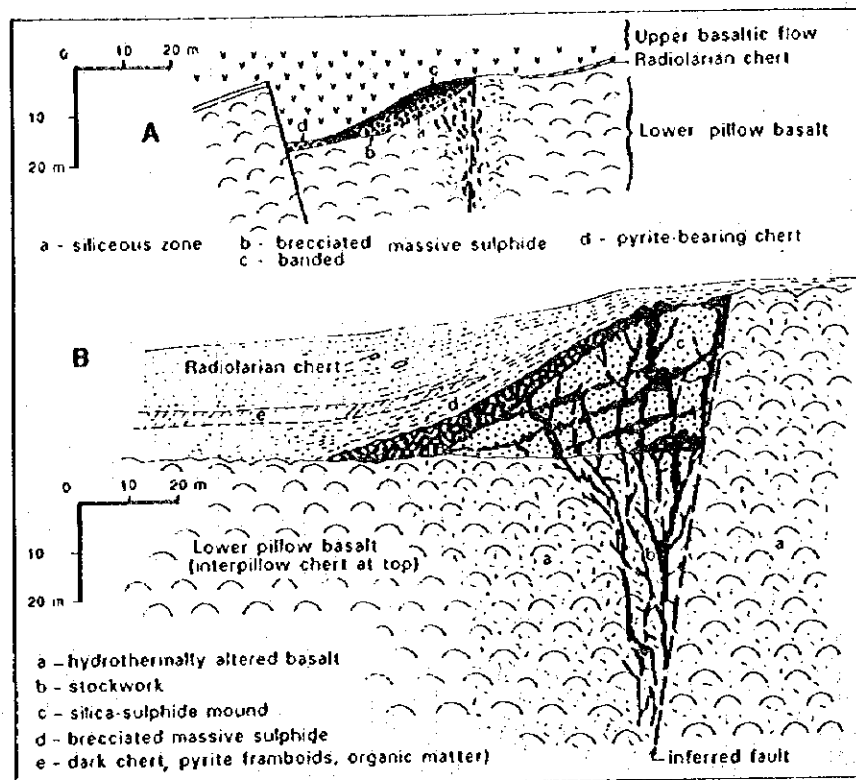


Line 800W

1000
900
800
700
600
500
400
300
200
100
0







(Lescuyer et al., 1988)

Fig.II-4-9 Schematic model of Daris and Rakah deposits

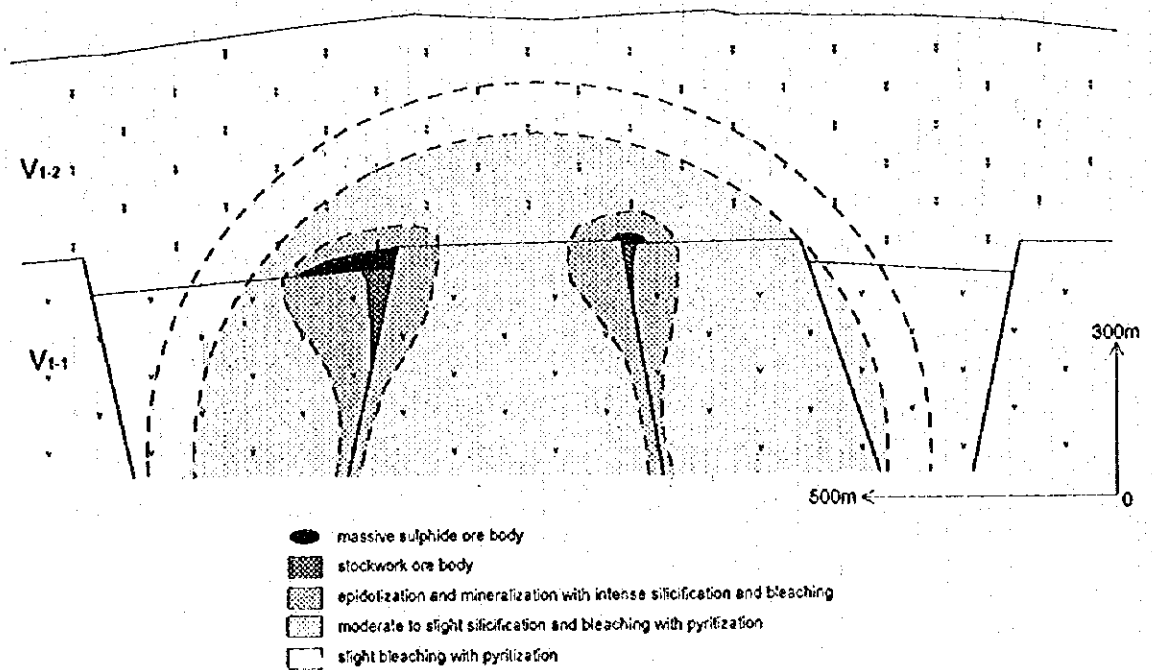


Fig.II-4-10 Schematic model of massive sulphide deposit in Central Batinah Coast

the idea that main fault is running in a north-south direction at the eastern edge of the body, in which the hydrothermal solution after being discharged, flowed towards northwestern direction while precipitating ore minerals and diffusing over sea floor.

The fact that intense chalcopyrite dissemination is observed in the Lower extrusive 2(V1-2) and on the hanging wall of massive ore, together with the fact that intense pyrite dissemination and silicification are also found in Lower extrusive 2(V1-2) at holes of G1 and G10, suggest that the mineralization in Ghuzayn had continued sometime after the formation of massive sulphide and was related to the early volcanic activity of Lower extrusive 2.

As for the alteration associated with mineralization, silicification, bleaching and epidotization are observed in this area. They are found in both sides of the foot wall and hanging wall and accompanied by pyrite dissemination, however, they are more intense in the foot wall side. In addition, their intensities are increasing as approaching towards massive ore bodies. Both, silicification and bleaching, are widely distributing around ore bodies and bleaching covers a slightly larger extension. These extents coincide almost with the area delineated as the high chargeability zone by TDIP survey. On the other hand, a epidotization appears in a limited extension near ore bodies. Epidote associated with mineralization is mainly forming veinlets together with quartz or calcite, which is accompanied by pyrite, chalcopyrite and rarely sphalerite. Massive epidote is in places observed beside the massive ore bodies and is sometimes accompanied by disseminations of pyrite and chalcopyrite as seen in the hanging wall of G5 hole. Difference in alteration can be observed between the two bodies. The Northern body is characterized by a more remarkable silicification and bleaching and the Western body shows is characterized by a more remarkable epidotization.

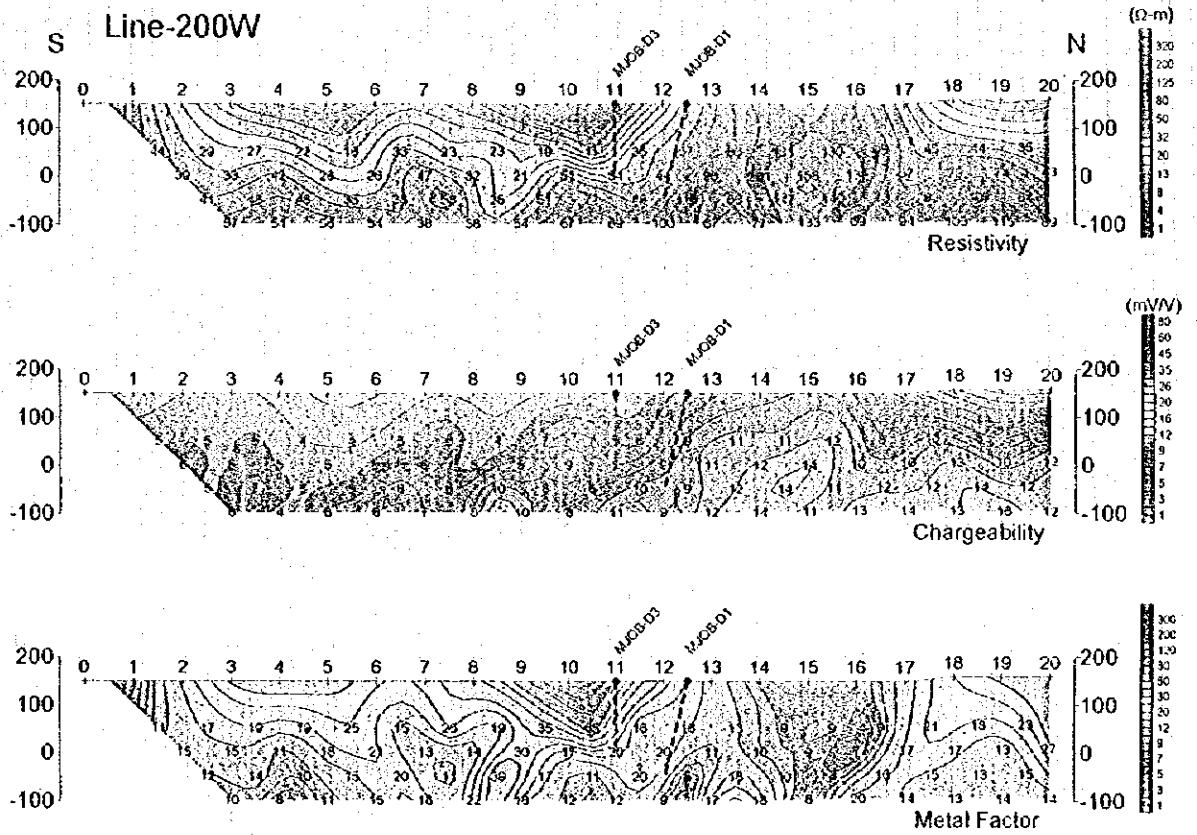
Based on above facts and considerations, a model of Ghuzayn deposits can be schematically made as shown in Fig. II-4-10.

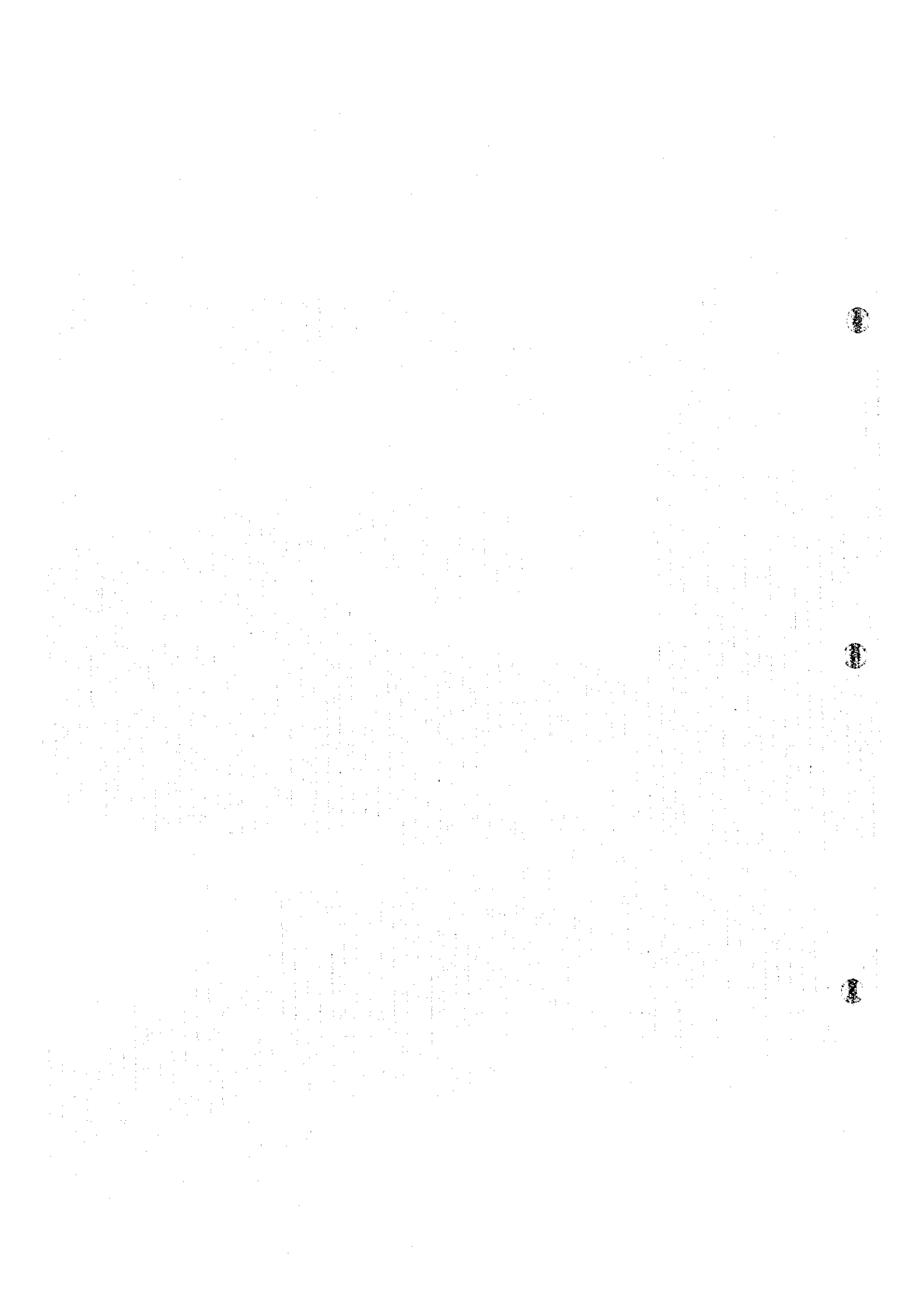
4-5-2 Daris area

Massive sulphide ore body could not be found in Daris area by the survey carried during this Phase. TDIP pseudo-sections including the crossing bore holes are shown in Fig. II-4-11.

Extensive high chargeability zone was detected by the TDIP survey in Phase I in the central part of the Daris area. Gossan and small massive sulphide ore bodies discovered by previous works are located in the southern edge of this high chargeability zone. Accordingly, TEM survey was carried out by using one loop around the known occurrences. The detected TEM anomalies were investigated by a drilling survey.

MJOB-D2 encountered an intense pyritization, however MJOB-D1 and D3 could not intersect any clear mineralization. The anomalies detected by TEM survey in the sites of MJOB-D1 and D3 are





considered to be due to fracture zones accompanied by clay and pyrite.

MJOB-D4 drilling was conducted to investigate the deep TEM anomaly detected near gossan. Since mineralization was encountered only in a shallow depth, it is inferred that the deep anomaly is probably due to fractures.

Since a high chargeability zone is seen widely distributed in Daris area, there is still a high possibility to find new deposits. However, ore bodies may be deformed by structural movements shown by the cataclastic texture in many parts of MJOB-D1.

4-5-3 Daris 3A5 area

The drilling survey of two holes was carried out to investigate the very low resistivity zone with moderate chargeability detected by TDIP survey of Phase I (Fig. II-4-12) to the northwest of gossan and massive sulphide ore bodies. The two holes could not intersect any mineralization, except a slight gossanization in MJOB-A1. The geology of both holes consist mainly of slightly weathered and strongly montmorillonized hayaloclastite in shallow depth and strongly chloritized hayaloclastite and pillow lava in depth. Finely fractured cores were obtained in most of the parts at shallow to middle depth of both holes. Judging from the results of drilling survey, the intense resistivity anomalies detected by TDIP is considered to be due to a strong montmorillonization and ground water filling fractures.

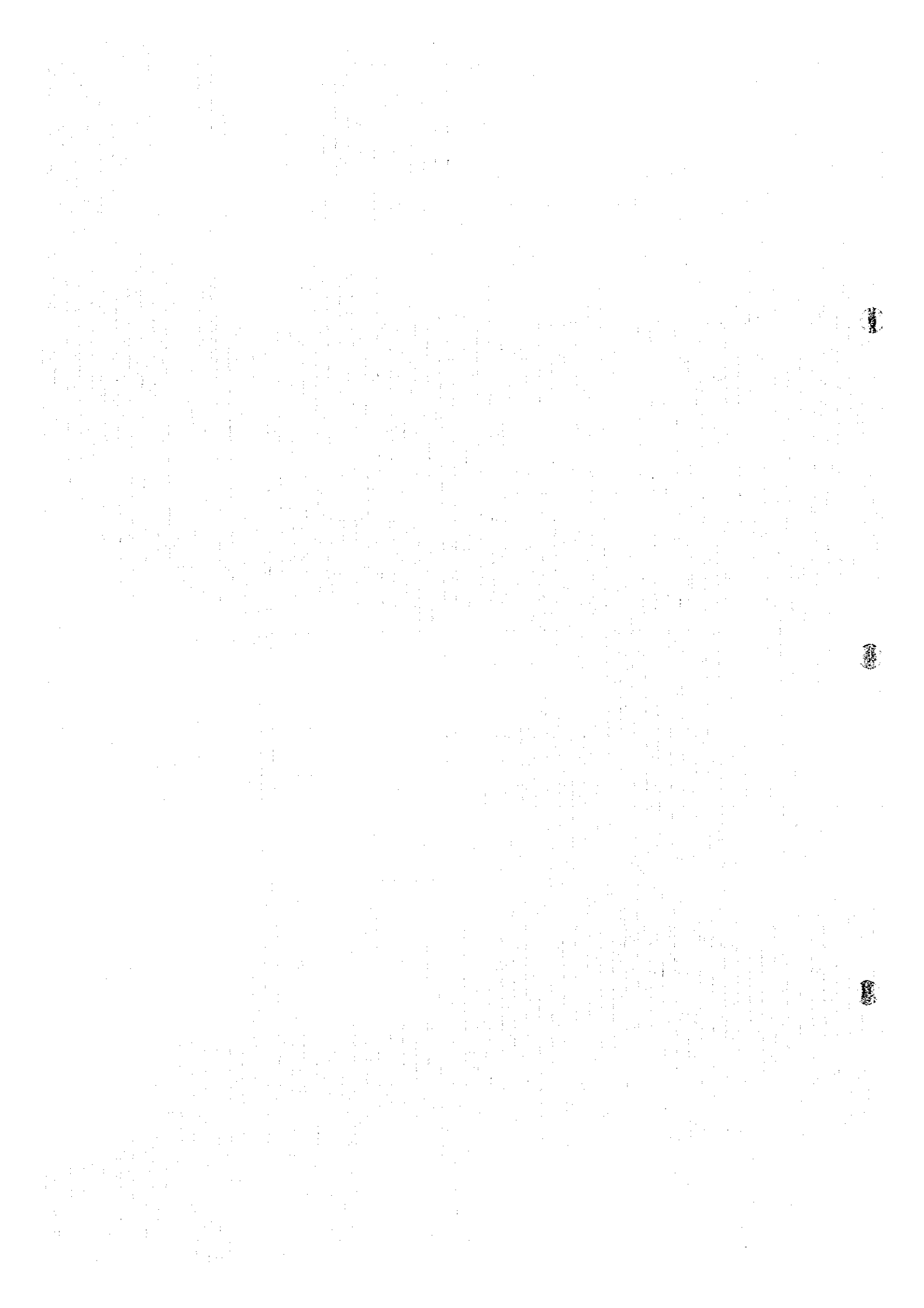
4-5-4 Daris North area

Extensive high chargeability and low resistivity zone was delineated by the TDIP survey in Phase I in the northern part of the Daris area. This anomaly which was confirmed by TEM survey, was further investigated by a drilling survey. TDIP sections including the crossing boreholes are shown in Fig. II-4-13.

The drilling was conducted in the center of TEM anomalies, however, no significant mineralization was encountered. In this hole, the Tertiary sedimentary rocks continued up to 131.85m before encountering Samail volcanic rocks, which is a calcareous sequence with intercalation of many mudstone beds. A considerable amount of pyrite were observed in these mudstone. These facts support the idea that the TDIP anomalies reflected the mudstone beds and pyrites in mudstone.

4-5-5 Fardah area

In Fardah area, TDIP survey in this phase delineated a remarkable low resistivity anomaly, however, it was not accompanied by high chargeability. Accordingly, only oxidized ore bodies were



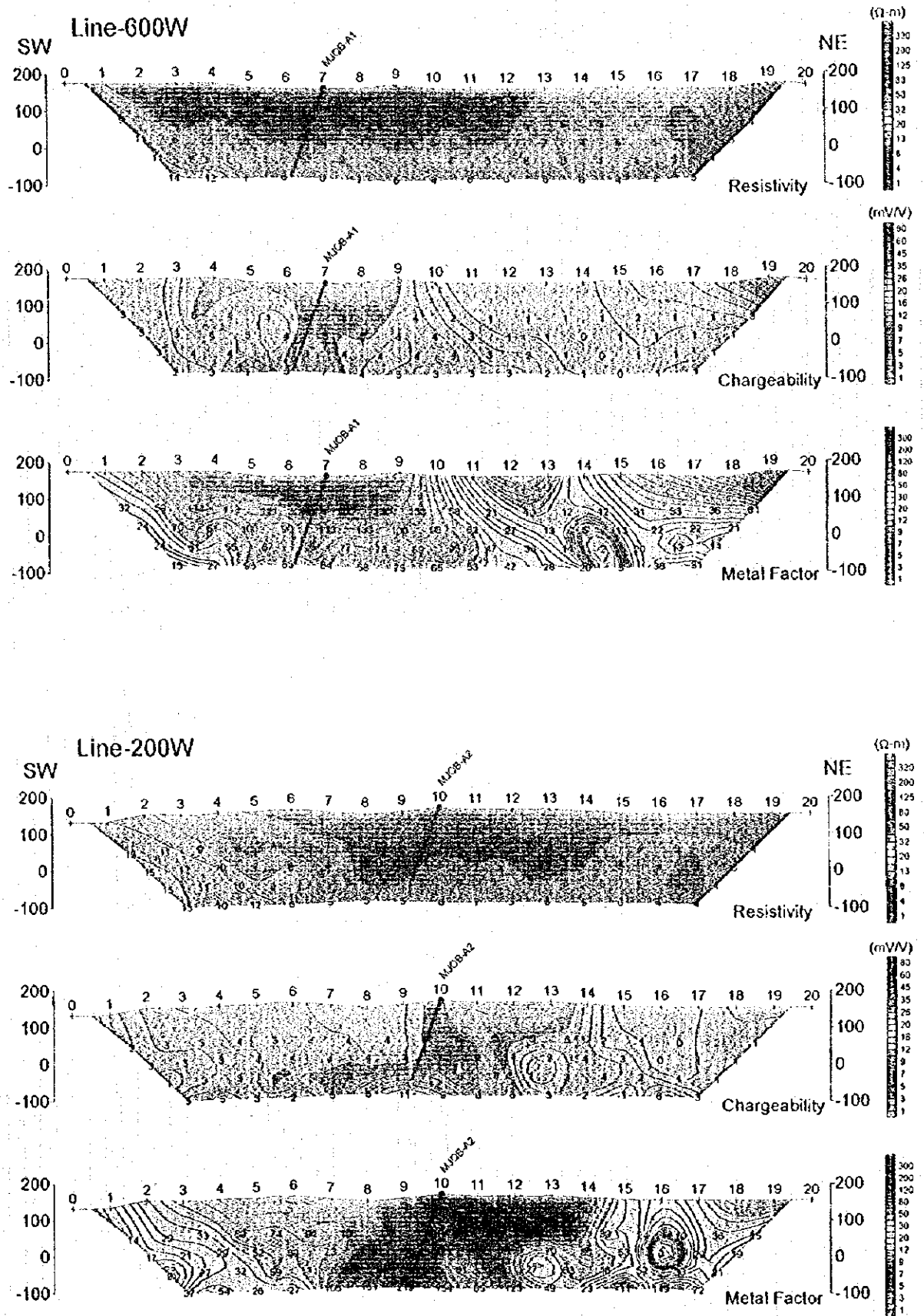
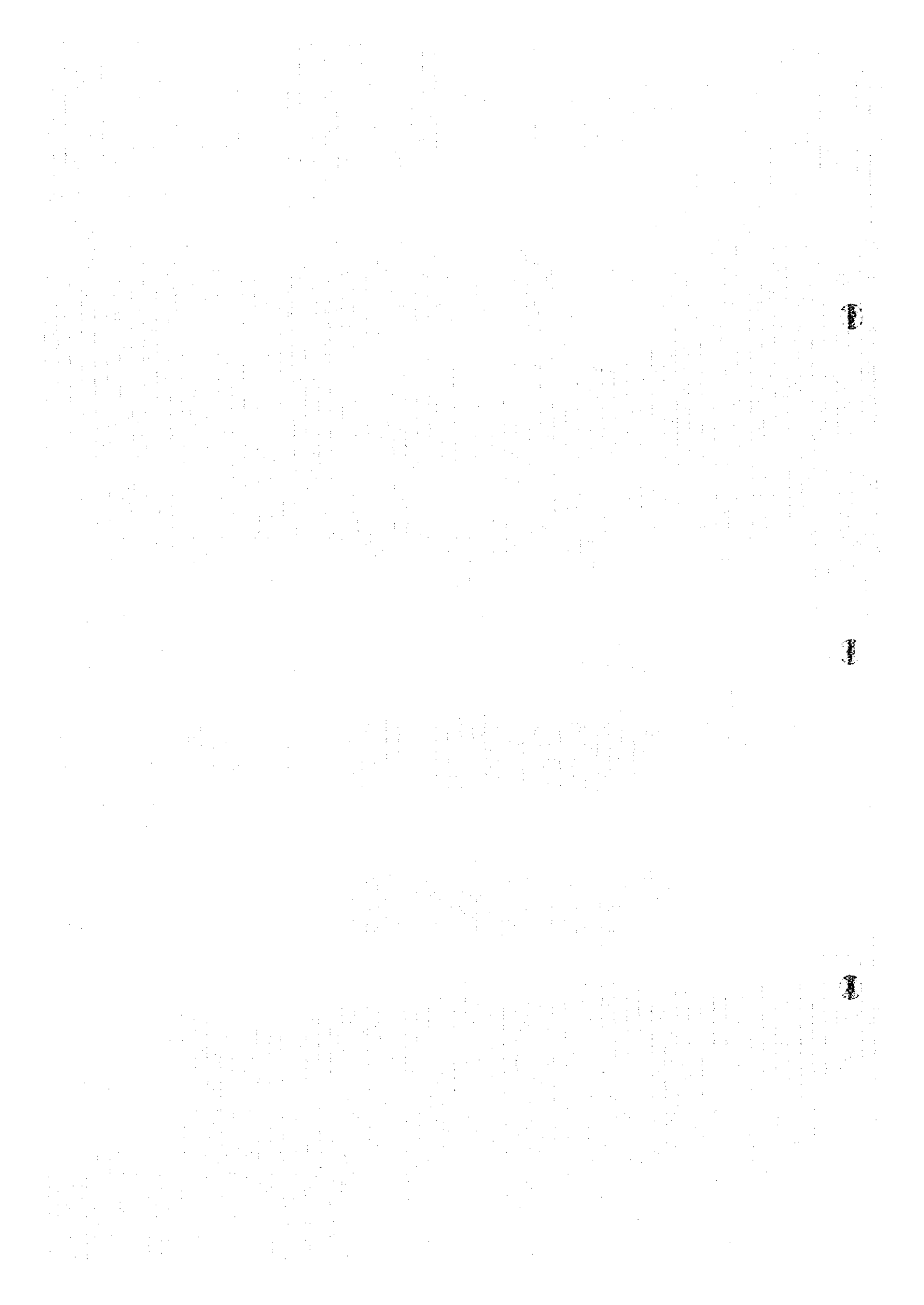


Fig.II-4-12 IP pseudo-section around bore holes in Daris 3A5 area



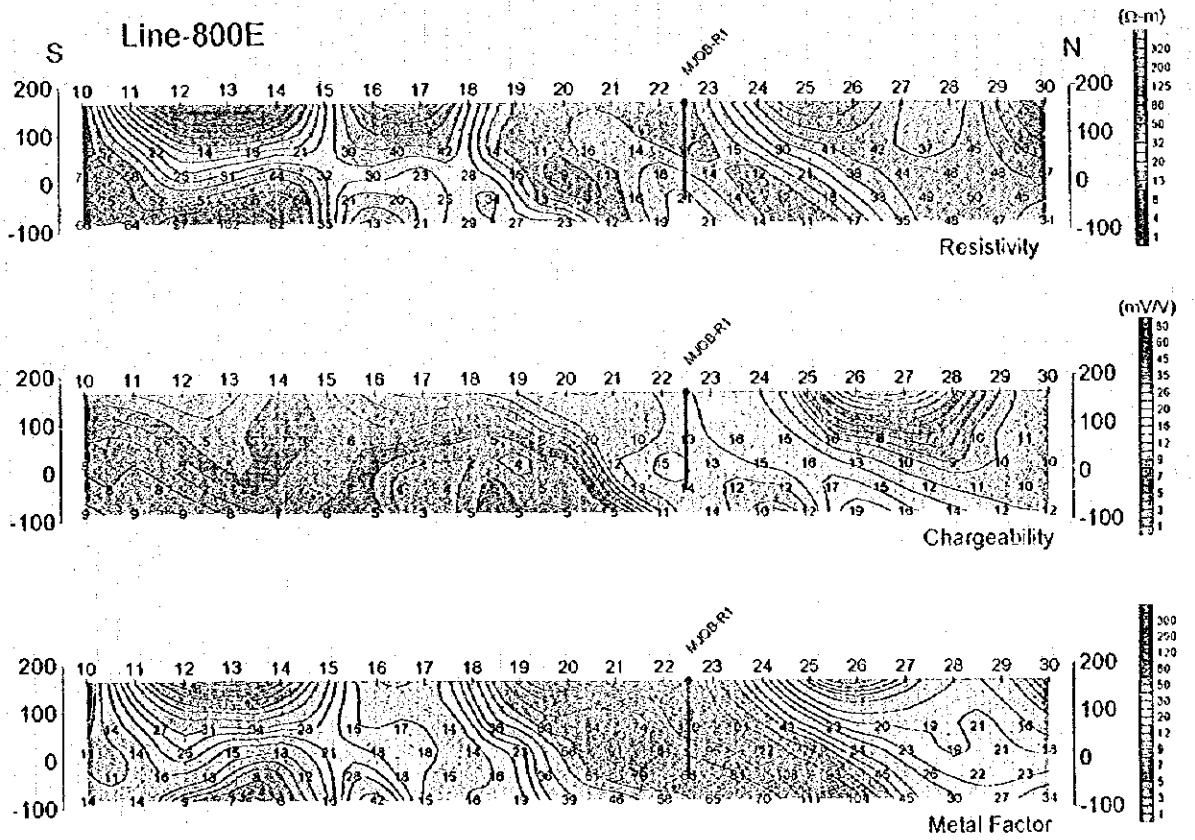
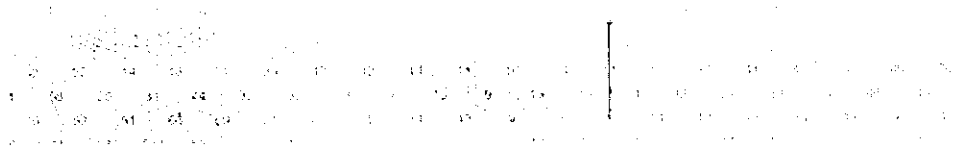


Fig.II-4-13 IP pseudo-section around bore holes in Daris north area

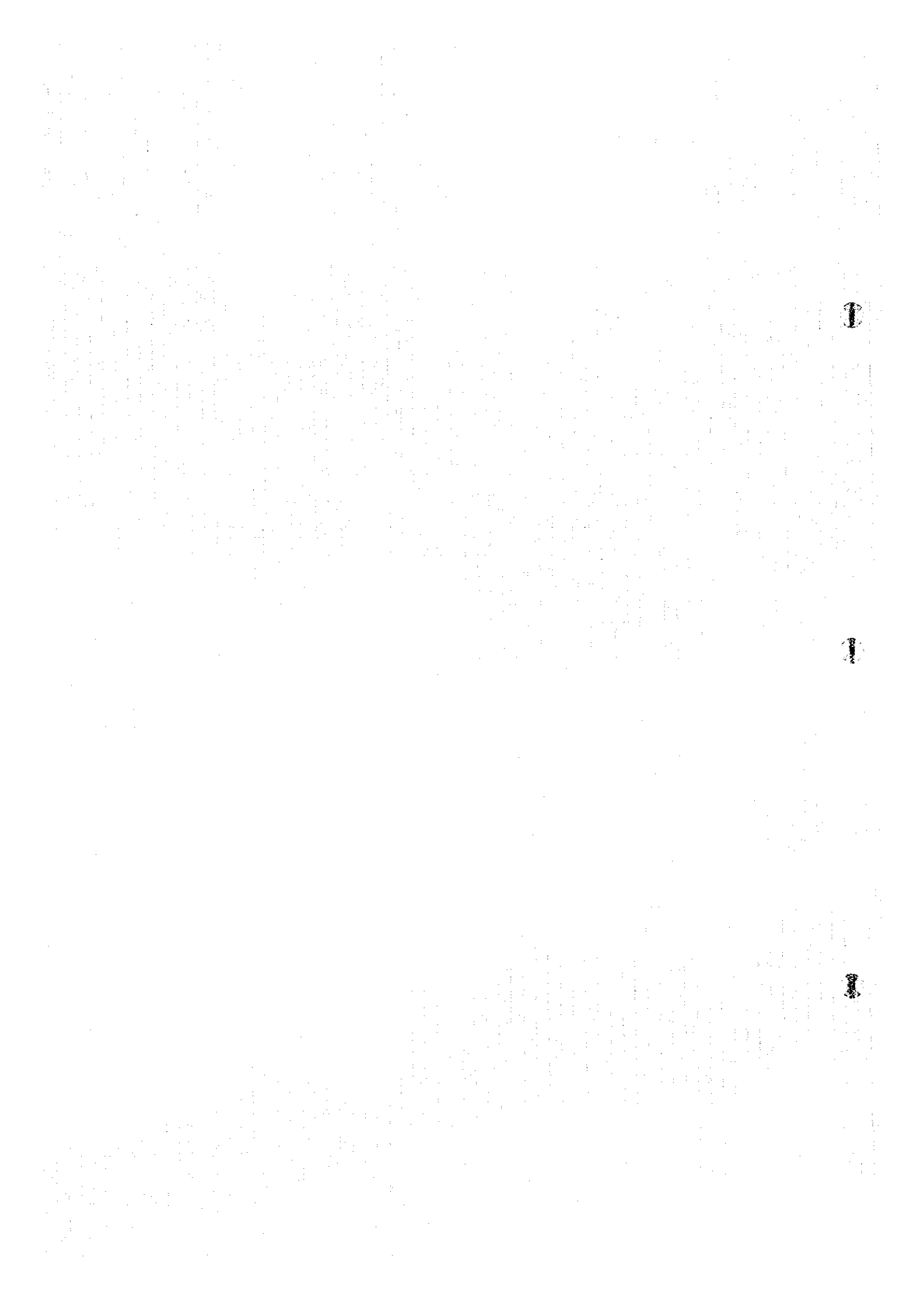
Line 8001





expected in the area. TEM survey was carried out to this anomaly and the detected TEM anomaly was investigated by a drilling survey. TDIP sections including the crossing boreholes are shown in Fig. H-4-14. Since no significant mineralization was intersected by this drilling survey, the low resistivity anomaly is considered to be due to mudstone beds of Tertiary formation unconformably underlying with Samail volcanic rocks. In addition, the gossan found in the Tertiary rocks seem to be formed by chemical weathering related to groundwater.

Because of the results in Fardah area and because same geologic and geophysical features were found in Sanah area, no drilling survey was carried out in Sanah area.



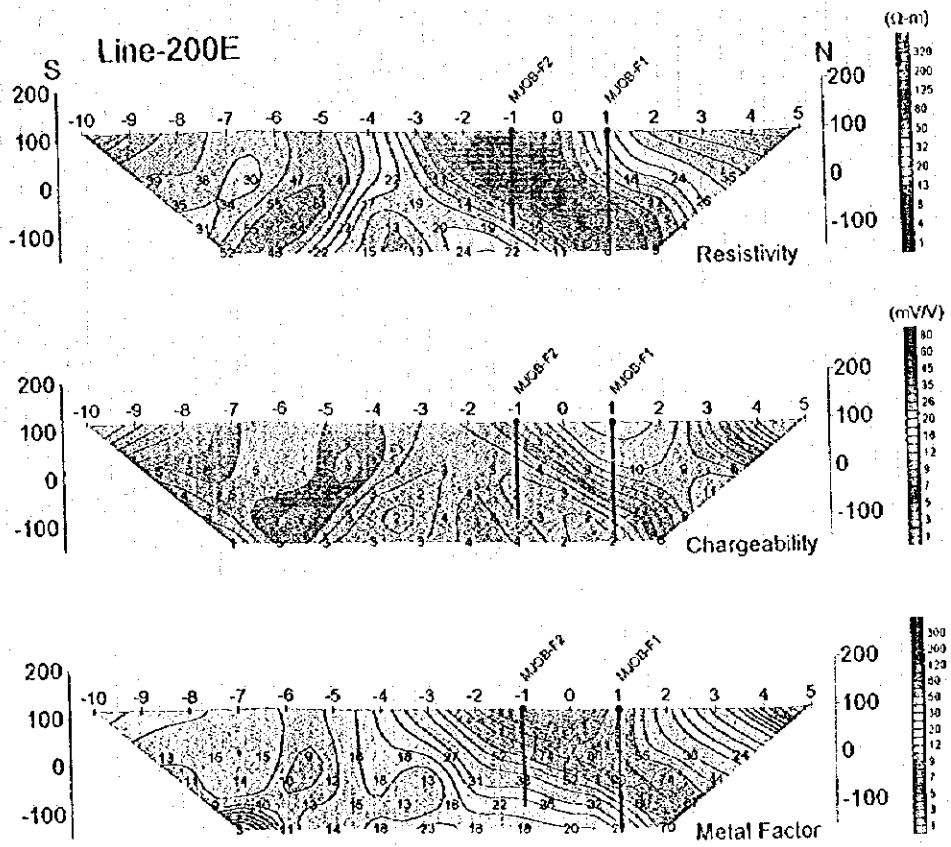


Fig.H-4-14 IP pseudo-section around bore holes in Fardah area

Line 200L

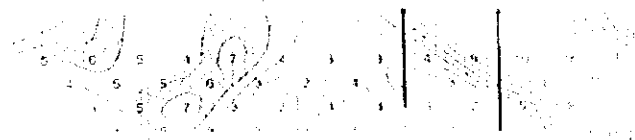


Figure 10-11



CHAPTER 5 DISCUSSION ON SUITABLE GROUND GEOPHYSICAL METHODS APPLIED TO MASSIVE SULPHIDE DEPOSITS

Based on the results of the ground geophysical surveys that we carried out not only during this year, but also in previous years in Sohar, we investigated on the suitable geophysical methods in order to implement an efficient exploration strategy in the search of massive sulphide deposits in Oman.

The massive sulphides distributed in Oman are of the Cyprus-type copper deposits, and which occur within the volcanic rocks conformed by basaltic pillow lava and associated to a stratigraphic control.

The selection of potential areas for massive sulphide deposits, can be achieved by first selecting the most suitable zones by tracing the pillow lava sequence by means of geological and airborne magnetic methods. The airborne magnetic method are useful to delineate demagnetized zones associated to mineralization.

The zones selected by the above methodology can be further investigated by appropriate ground geophysical methods in order to delineate in more detail areas with high potentiality. The results of the geophysical methods can be finally confirmed by a suitable exploratory drilling program. Fig. II-5-1 illustrates a flow diagram for an efficient exploration strategy.

In Oman, one of the main difficulties to carry out mineral exploration is that the very wide area are covered by Quaternary sediments, and in this respect, it is important for future exploration works to effectively investigate blind deposits under the sediments. In particular, the flow chart described in Fig. II-5-1 illustrates the geophysical techniques that can be effective to find new deposits.

5-1 SELECTION OF GROUND GEOPHYSICAL METHODS

As illustrated by the schematic model for massive sulphide deposits in Central Batinah Coast (Fig. II-4-10), the massive sulphide deposits are also accompanied by sulphide dissemination. On this basis, the selection of the appropriate ground geophysical method should take into account not only the physical characteristics of the massive sulphide deposit but also the disseminated sulphides and their corresponding scale.

Flow for massive sulphide deposits exploration in Batinah Coast

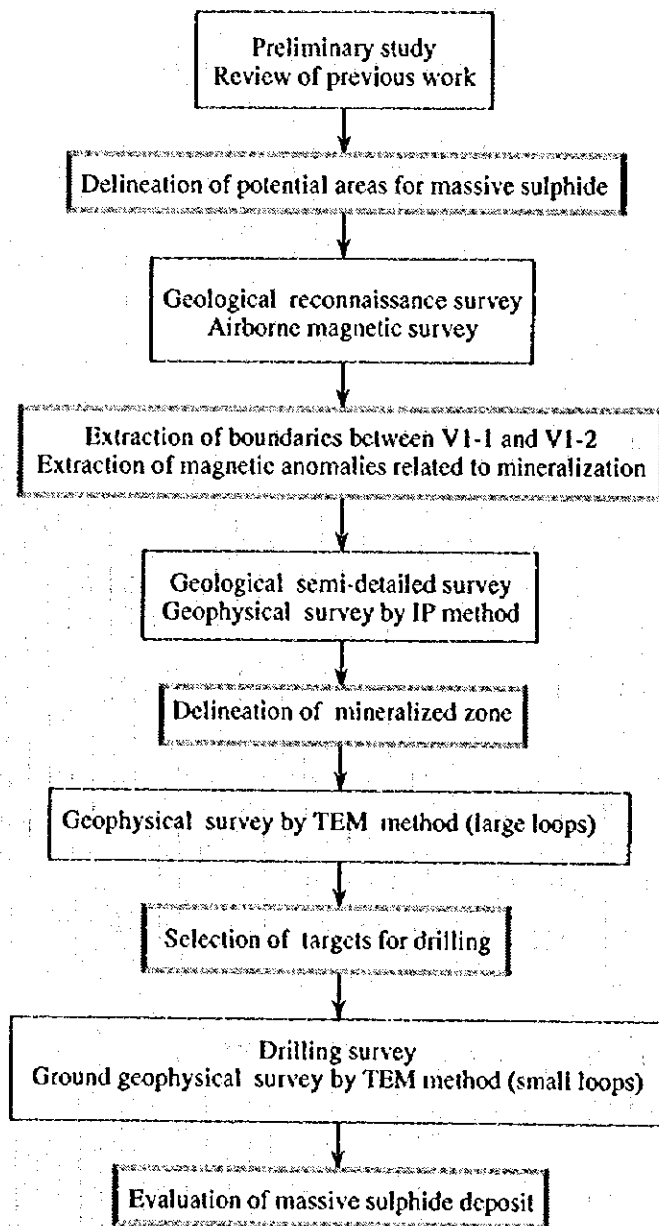


Fig. II-5-1 Flow for massive sulphide deposits exploration in Batinah Coast

In relation to the electrical properties of sulphide minerals massive deposits, it can be mentioned here that they present high chargeability and high conductivity (low resistivity). As the amount of sulphides increases, bigger electrical contrast differences can be detected between mineralized and non-mineralized zones.

For the case of exploration of Cyprus-type deposits in Oman and if we think of the scale of the deposits, it is quite complicated to find out directly massive sulphide deposits from the wide zone covered by Quaternary deposits. As such is the case, it would be also important to include within an exploration program, the search of disseminated sulphides which can be observed within a wide scope.

According to the flow diagram of Fig. II-5-1, the IP method is useful to search for high chargeabilities associated with sulphide mineralization. Simultaneously, underground resistivities are also measured. To confirm the IP results and to obtain resistivity in more detail and at deeper levels, the TEM method is also recommended after the IP survey results are known.

Among these two geophysical methods, IP can be useful to delimit the extension of the mineralized zone, by measuring chargeability as an electrochemical phenomena of the disseminated sulphide mineral. As mentioned previously, the IP method detects also low resistivity and as a result, another parameter called metal factor can be calculated. The metal factor is simply the ratio between chargeability and resistivity. High metal factor values are related to high possibilities for favorable mineral potential deposits, because higher contents of sulphide minerals can be associated to higher chargeabilities and lower resistivities of the rock.

Other geological environments which indicate also low resistivity, such as sedimentary rocks, e.g., mudstone, and layers containing saline water, can be distinguished from sulphide minerals signature by their low chargeability, which implies low metal factors. Accordingly, the IP method which is able to detect chargeability within a wide range can be useful to infer the disseminated sulphide distribution at a wide scale. At the same time, the ability to detect low resistivity distributions to extract high metal factors can be helpful to delineate even more the possibility to detect any existing sulphide mineralization within the area.

On the other hand, one of the weak points of the IP method is the ability to measure the IP parameters only along lines, however, if deeper exploration depth is wanted due to a deep target, the distance between electrodes can be increased longer, but as this is done, the scope of lateral influence gets wider, and as a result, the resolving power decreases more and becoming in this way, more difficult to decide the place of the source of the anomaly. On the contrary, by the TEM method although only the information of resistivity can be obtained, its value can be obtained directly below the observed point. To this it can be added that the sensitivity to extremely low resistivity bodies is higher as compared to another geophysical method.

Specially in Oman, the TEM method can be very effective, because in this case the host rock is compact and hard and therefore, a big contrast in resistivity can be seen if compared to the massive sulphides. The TEM response detected by the TEM method from hard rock is small and as such, a big TEM response can be expected from a massive sulphide deposit.

According to the above mentioned and for the case of the Cyprus-type deposits, massive sulphide targets can be discovered by first applying the IP method in order to extract a wide area where a wide high chargeability distribution with low resistivity can be detected under sediments, and as a second step, distributions with high chargeability and low resistivity values can be more precisely investigated by TEM method to delineate the most promising targets as defined by the most prominent TEM responses.

5-2 RESULTS OF APPLICATIONS

5-2-1 Previous Survey in Sohar Area

From 1985 to 1990 geological regional surveys as well as detailed exploration surveys were carried out for about 6 years in the area of Sohar of the Sultanate of Oman. Within this period and at the beginning of the exploration survey, every kind of ground geophysical survey was tested, and as a result, the IP and TEM methods resulted specially effective for the exploration of massive sulphides in the area. In what follows and as a matter of example, we will very briefly mention the results obtained by using the above mentioned ground geophysical methods applied in Aarja and Bayda deposits and its surroundings, which had been discovered at the beginning of the survey.

Fig II-5-2(1) and II-5-2(2) shows the results obtained by the IP survey method near Aarja and Bayda deposits. As it can be clearly seen in these figures, both of the deposits are located in the edge of a high chargeability distribution and high metal factor (over 40). Around the deposits, there can be seen a zone of high chargeability distributed in a wide area.

Fig. II-5-3 shows in a plan map, the TEM responses of one of the results obtained by the TEM method applied around the Bayda deposit. In this map, high TEM responses are seen towards the south and north central direction of what is now the deposit. As compared with the result obtained by the IP method, the anomaly detected by the TEM method was able to delineate the location of the deposit in a more precisely way. It shows then, that the TEM method is effective to locate the massive sulphide deposit.

5-2-2 Geophysical Survey Results in Ghuzayn area

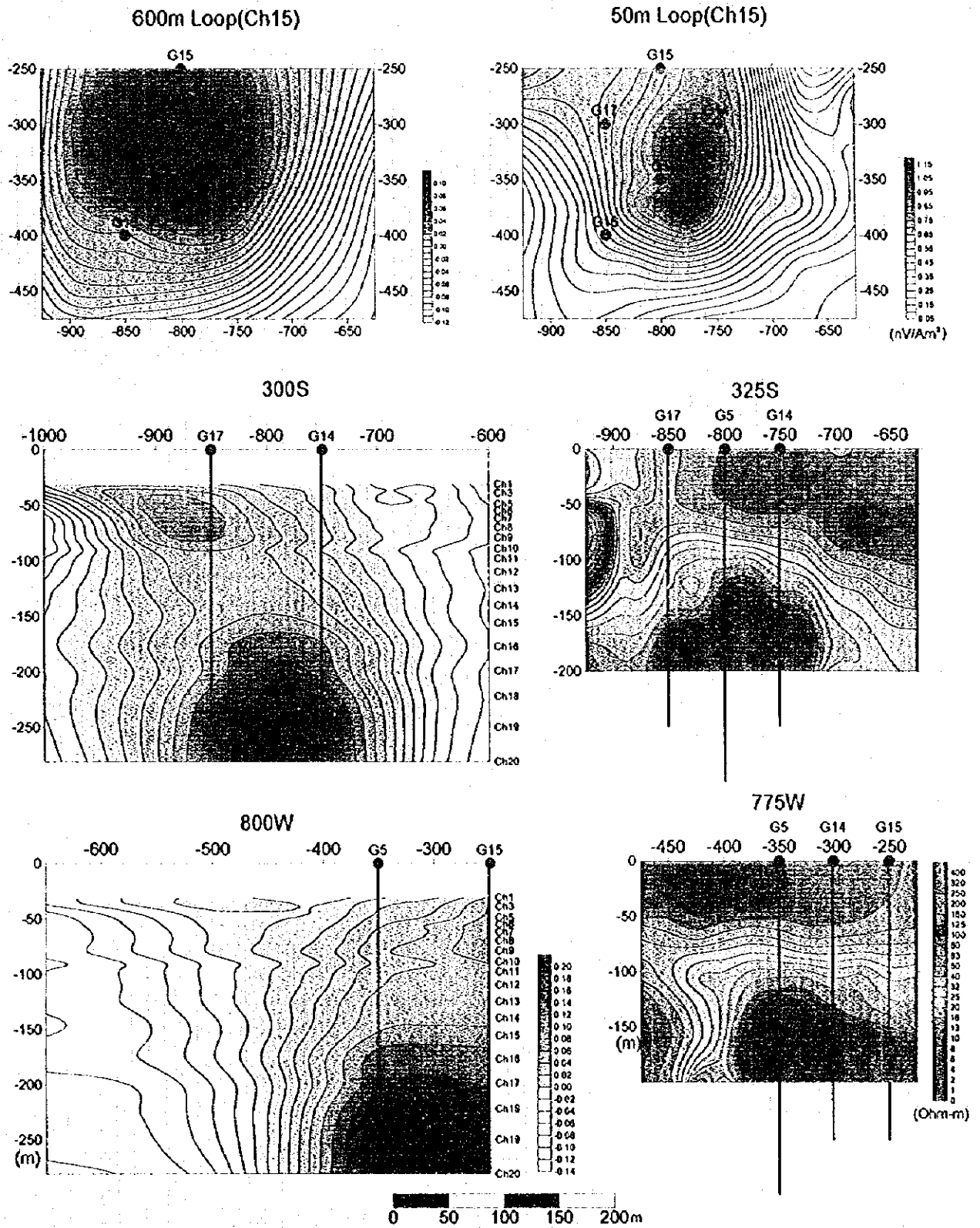


Fig.II-5-5 TEM anomaly comparison map with 50m and 600m loop

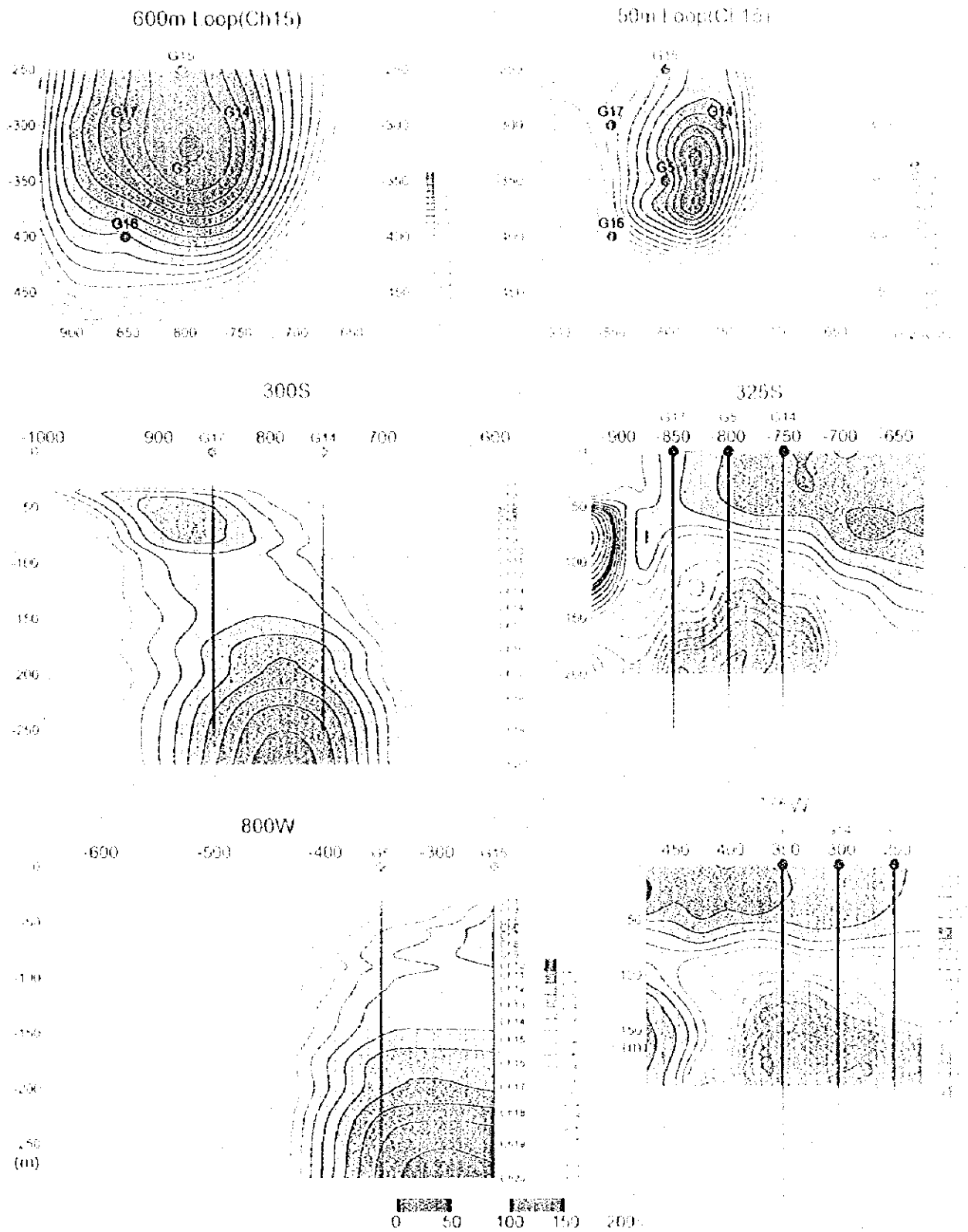


Fig B S S IEM magnetic comparison map with station ID (96m to 100m)

1

1

1

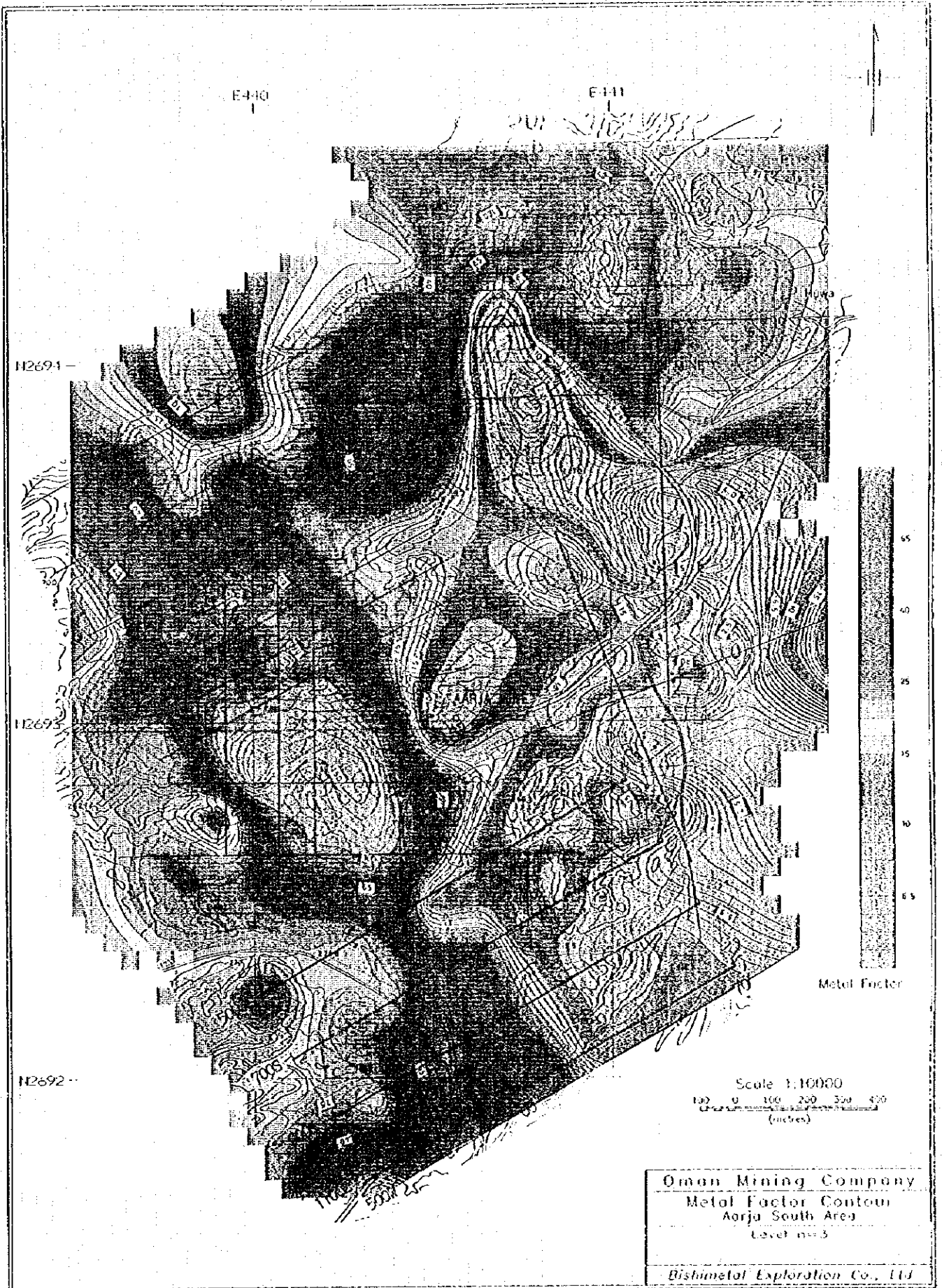
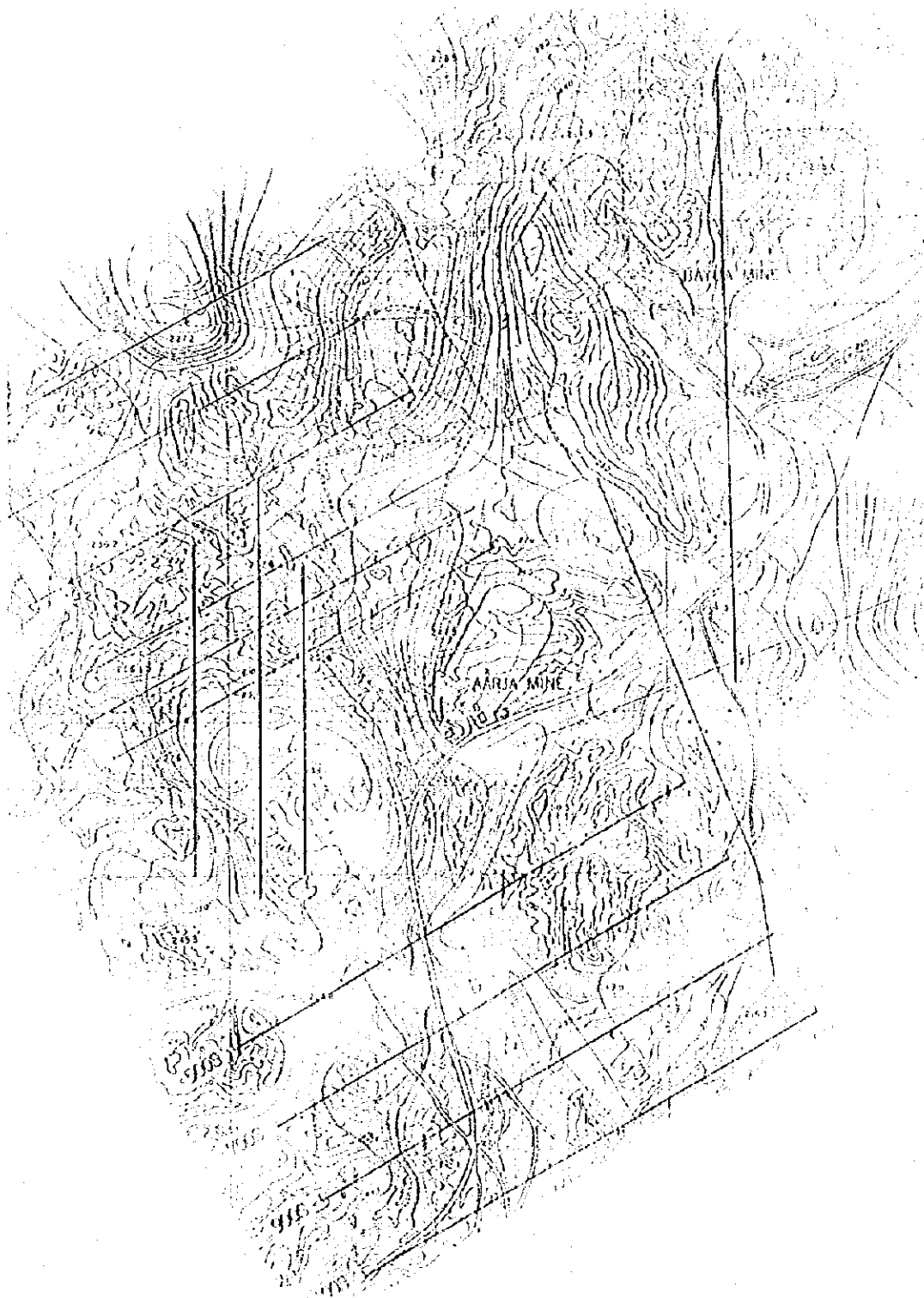


Fig. II-5-2(2) IP result plane map near Aarja and Bayda deposits



1

2

3

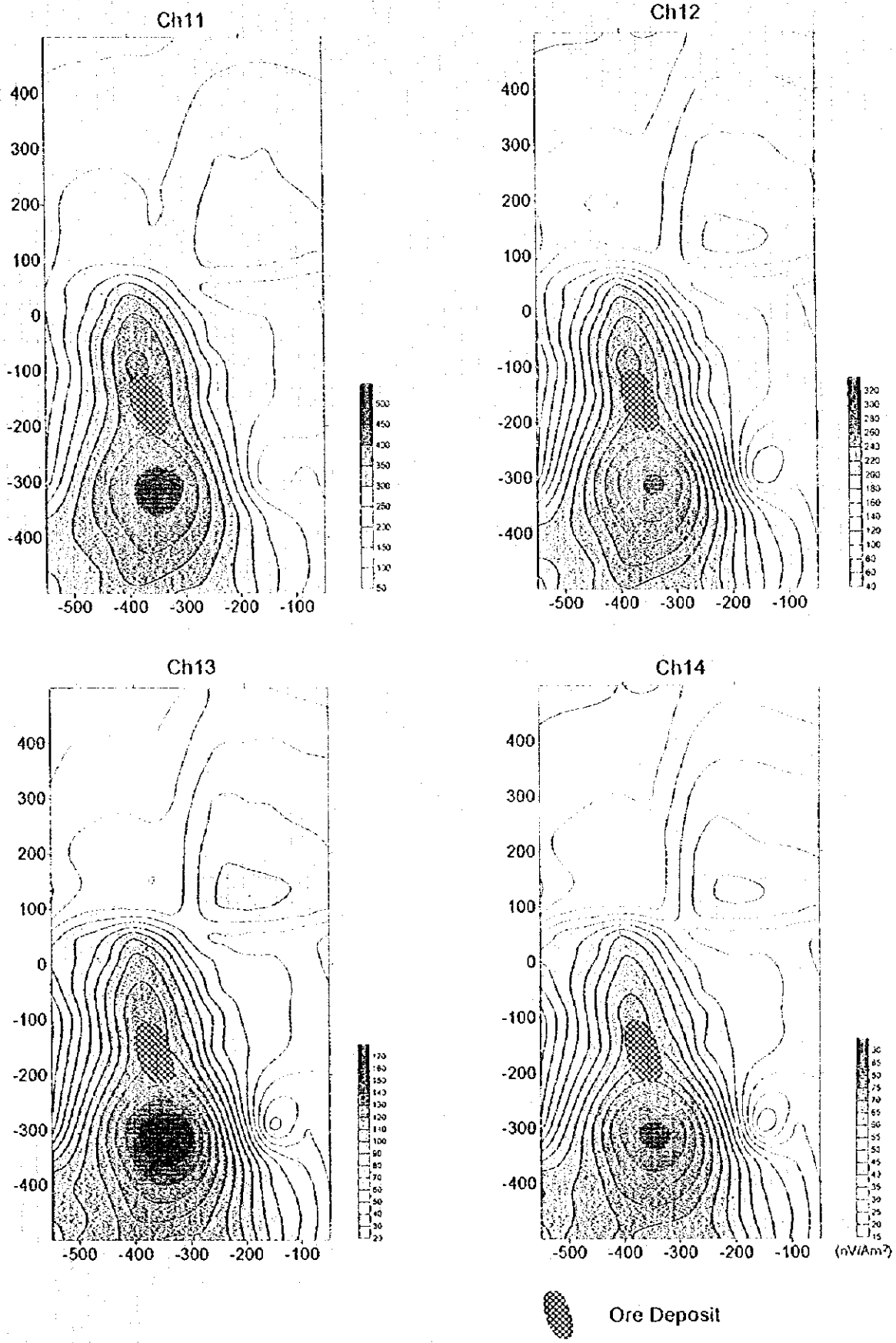


Fig.II-5-3 TEM response plane map in Bayda deposit



In Ghuzayn area an IP survey was carried out during the first year of the project. Based on the IP results, a TEM survey was carried during the second year of the project. As a result of these geophysical investigations, drilling exploration carried out around the detected geophysical anomalies, discovered new massive sulphide deposits.

(1) IP Survey Results

Fig. II-5-4 shows the results in a plan map of resistivity, chargeability and metal factor distributions obtained from the IP survey. The exploratory drilling carried during this year's survey indicated good agreement with the high chargeability anomalies and massive and disseminated sulphide mineralization encountered in the boreholes.

The confirmed Western and Northern orebodies (Fig. III-1) are located in a low resistivity zone with high chargeabilities, which implies that probabilities to discover sulphide mineralizations can be high in places where metal factors resulted with high values.

(2) TEM Survey Results

The TEM survey was conducted by taking into consideration the location of anomalies extracted by means of high metal factors detected around the central area of the zone where the IP survey was carried out. The location of the area where the TEM transmitter loops were deployed as shown in the Fig. II-5-14.

Fig. II-3-13 summarizes in a compiled map the results obtained from the TEM survey. According to the results, five TEM anomalies, including the Western and Northern orebodies, were detected in the area.

Since outside of this anomalies, disseminated mineralization was intersected by the drilling exploration, it is very likely that three of the above mentioned five anomalies find massive sulphide deposits with a high probability of success.

5-2-3 Guidelines for Future Geophysical Exploration Surveys

According to the ground geophysical results obtained in Oman for the exploration of Cyprus-type massive sulphide deposits, the first step towards the search of these deposits is the utilization of the IP method to cover a wide range. The distribution of prominent IP anomalies permits the extraction of a possible mineralization, which in turns, leads to the second step, i.e., the implementation of a TEM method within the areas delineated by IP method.

The results of the TEM survey add more probabilities to discover massive sulphide deposits by clarifying the distribution of high TEM responses.

In this survey and in order to increase the speed and efficiency during the survey, it was selected a large fixed transmitter loop with a receiver moving within the area. On the other hand, through tests carried out, it was found that the lateral and vertical resolution of the measured data can be improved by using loops small to some extent. The data processing for the case of small loop configurations is also less complicated.

The above mentioned fact can be further illustrated by the Fig. II-5-5, which shows a comparison of the TEM results around the borehole G5 by means of large configuration loops (600 X 600m) as well as small central loop (50 X 50m) soundings.

According to the TEM responses detected by the small loops, it appears evident that the massive sulphide becomes thin around the borehole G16 and in G17 where the TEM responses suddenly become weaker.

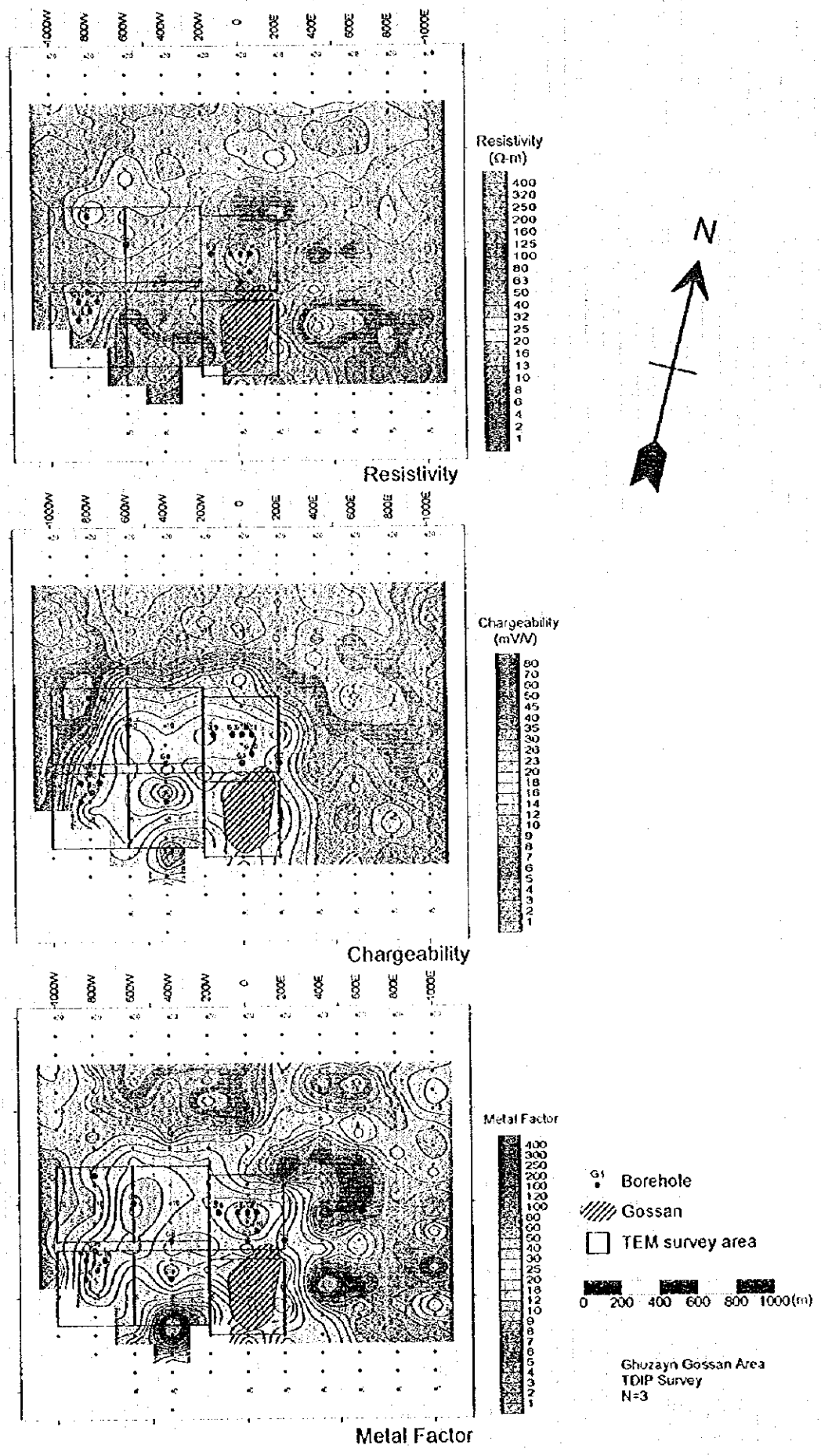


Fig.II-5-4 IP result plane map in Ghuzayn gossan area

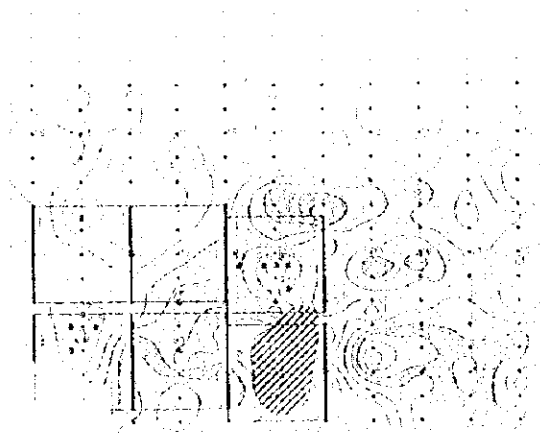


Figure 1

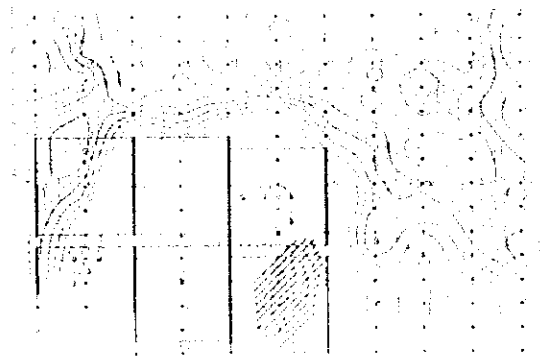
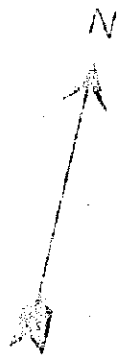


Figure 2

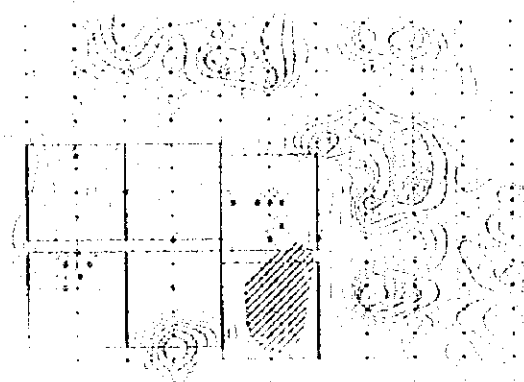
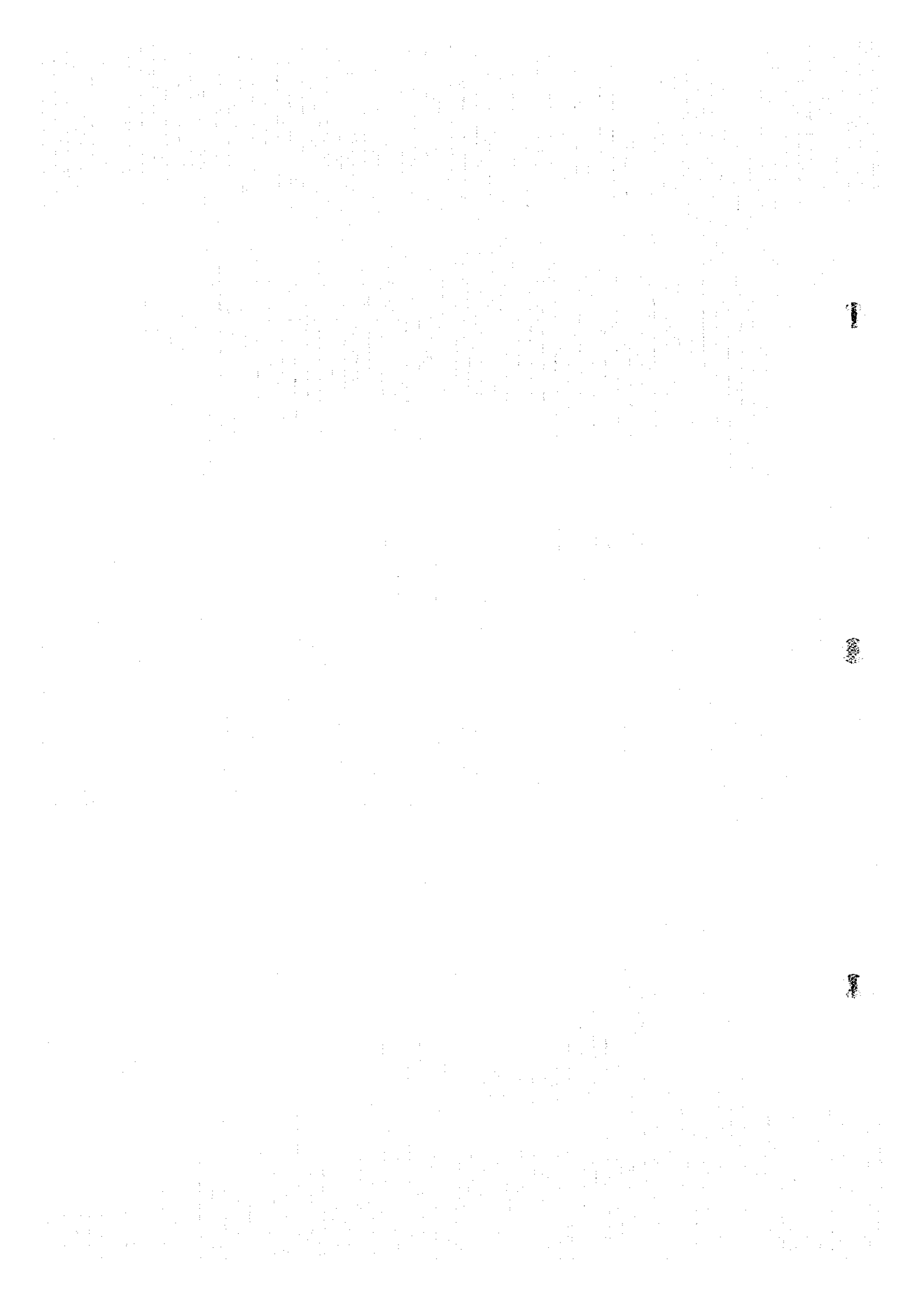


Figure 3

Figure 1, 2, and 3 show the same area with different grid patterns.



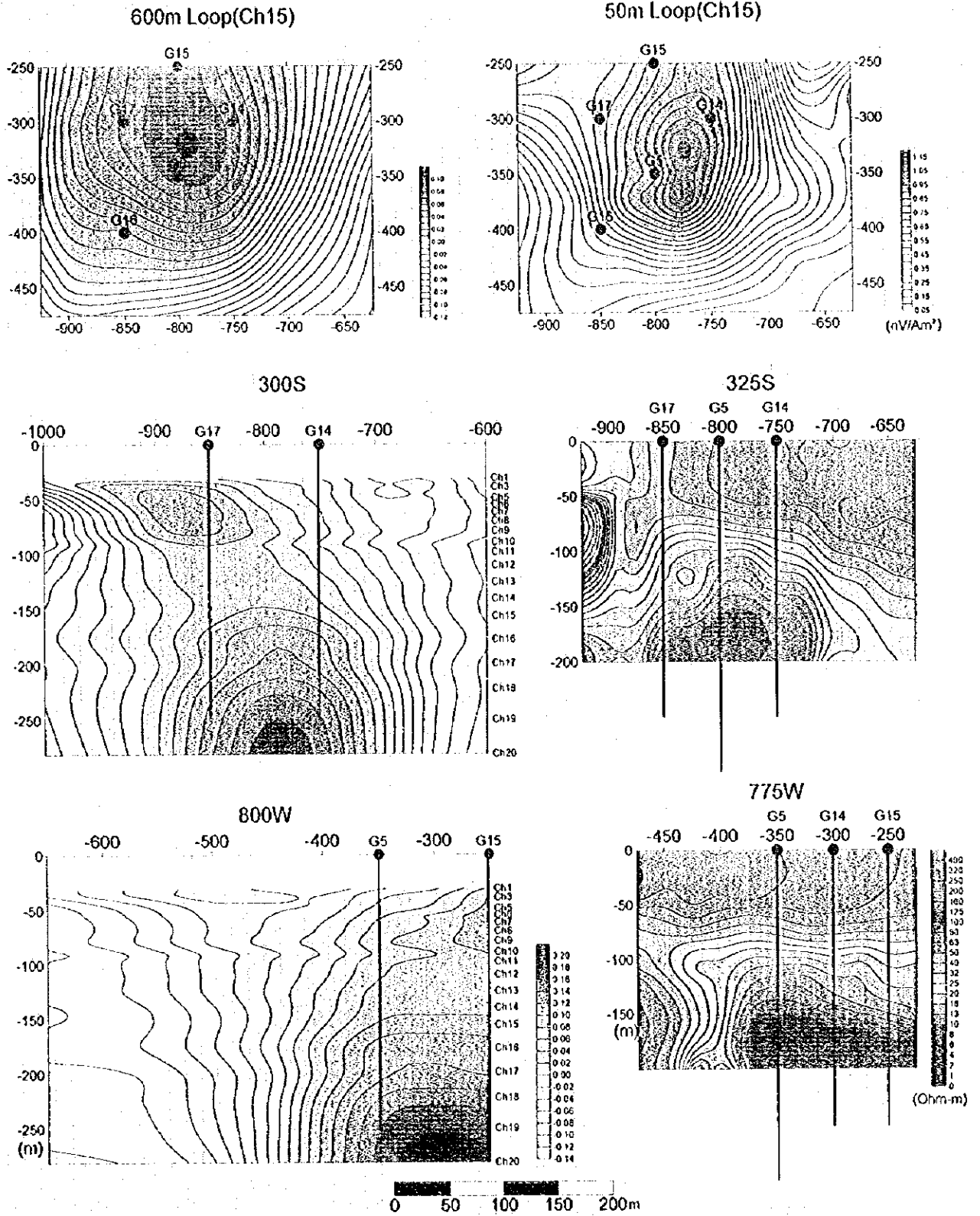


Fig.H-5-5 TEM anomaly comparison map with 50m and 600m loop

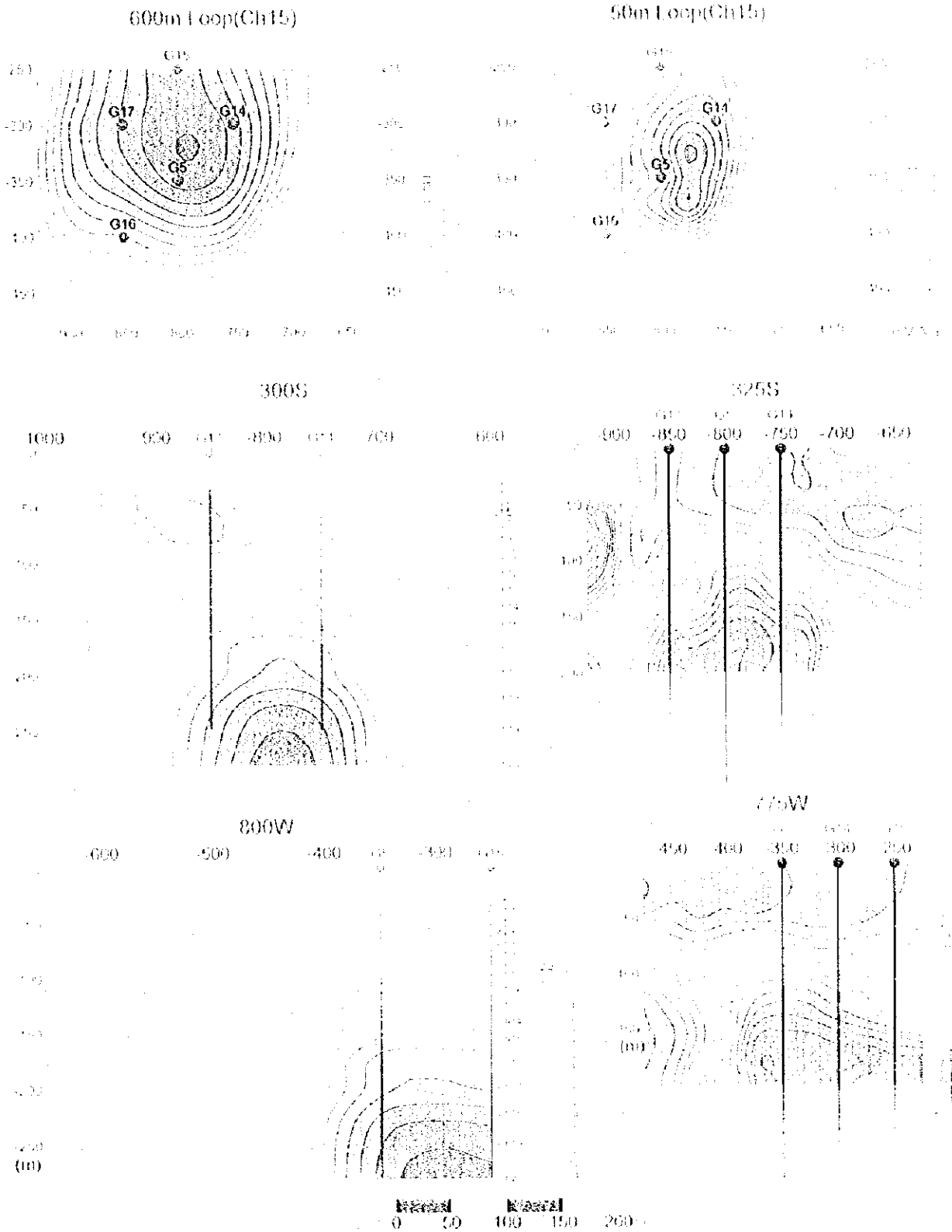
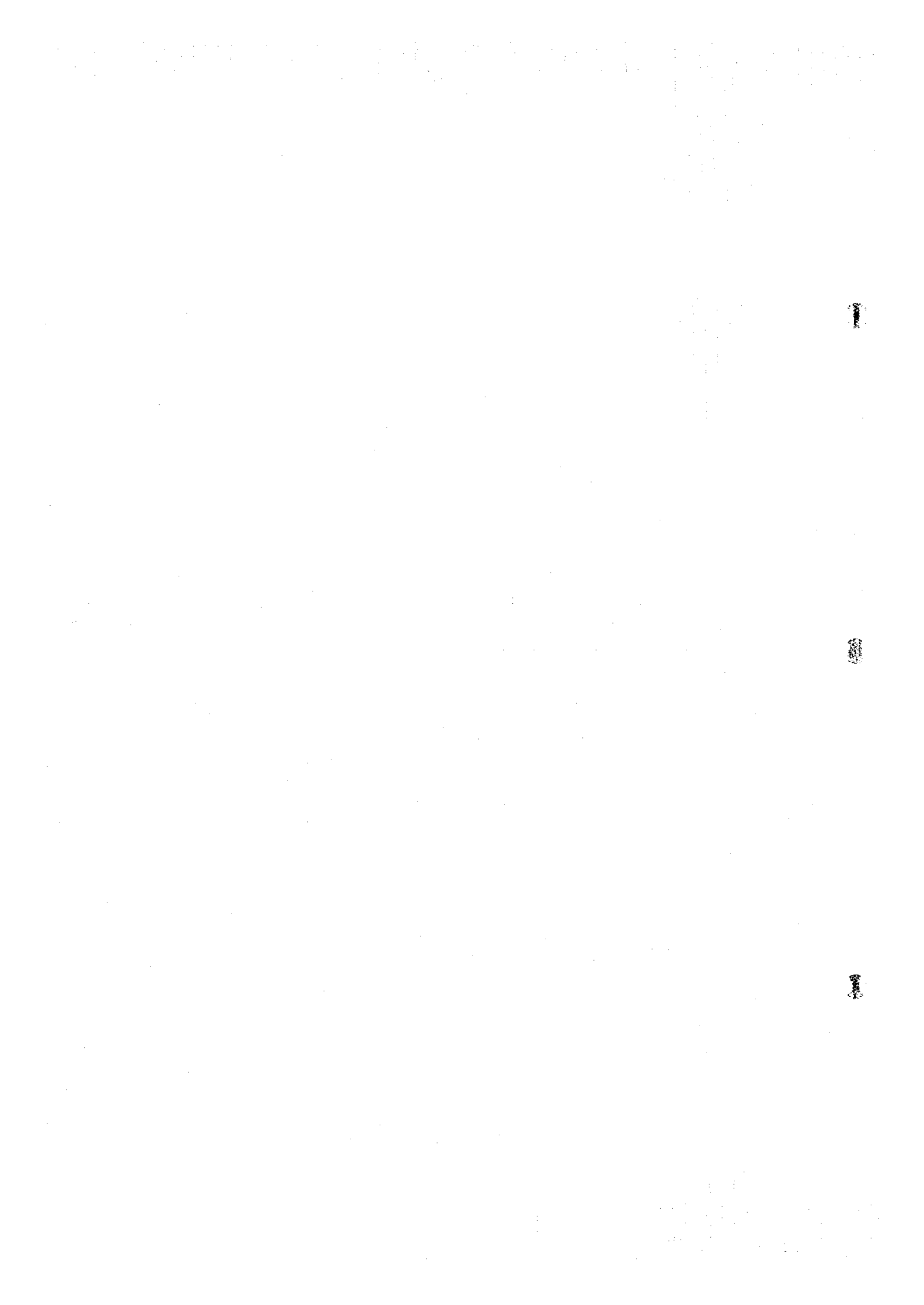


Fig. 10. S11 Magnitude comparison with 600m and 50m loops



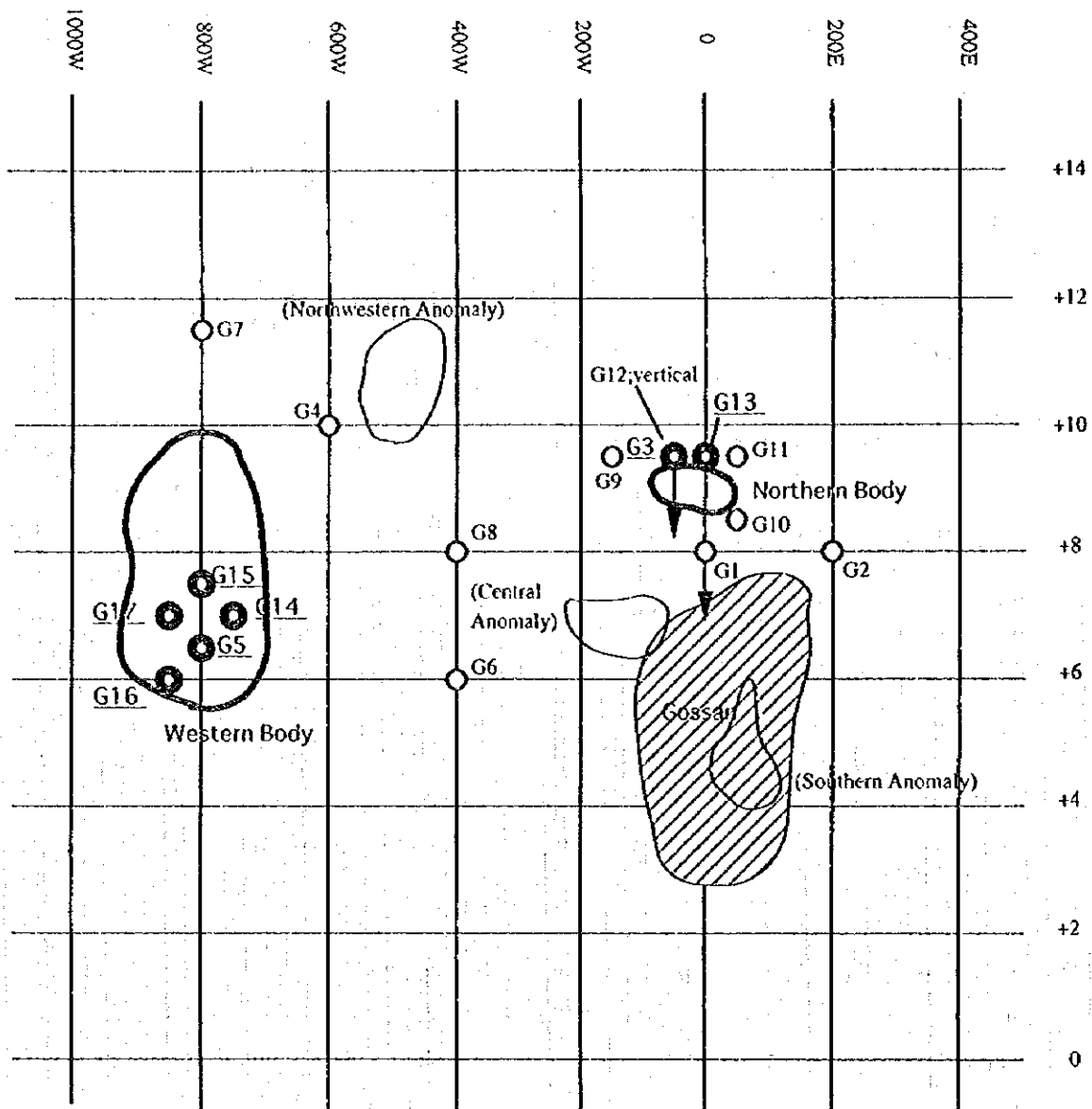
PART III CONCLUSIONS AND RECOMMENDATIONS



CHAPTER 1 CONCLUSIONS

The survey results can be summarized as follows:

- (1) Drilling survey conducted in Ghuzayn area intersected massive sulphide bodies in two places, i.e., in the northern and western part. The Northern body found to the north of gossan, shows a maximum core length of 7.95m with average assays of 4.66% Cu in MJOB-G3 hole. The Western body found to the west of gossan, shows a maximum core length of 37.1m with average assays of 1.88% Cu in MJOB-G14 hole.
- (2) TEM survey in Ghuzayn area highlighted the extension of massive sulphide ore bodies which were intersected in two places by drilling conducted in this Phase. The TEM data show also that the Western body has an extension of 150m wide in east-west direction and 300m long in north-south direction and that the Northern body extends 150m wide in east-west and 100m long in north-south. In addition, TEM data indicate also interesting anomalies which may correspond to high potential locations for massive sulphide mineralization in three places.
- (3) In Doqal area, TEM survey was conducted in order to investigate the high metal factor zone detected by TDIP. Since the TEM anomalies extracted in the area correspond well to the high metal-factor zone, it became clear that this area may have a high potential for mineralization of massive sulphide.
- (4) Because of the thick coverage of Quaternary sediments, a ground geophysical survey seems to be the most important and effective tool for the exploration of copper deposits in Oman. According to the survey of two years in Central Batinah Coast for the exploration of Cyprus-type massive sulphide deposits, the first step towards the search of these deposits is the utilization of the IP method to cover a wide range. The distribution of prominent IP anomalies permits the extraction of a possible mineralization, which in turns, leads to the second step, i.e., the implementation of a TEM method within the areas delineated by IP method. In addition, the effectiveness can be increased by conducting complementary TEM surveys by means of small loops (50m x 50m) along with the drilling survey in order to delineate in more detail the extension of ore bodies and allocate better the drilling targets.



-  Ore bodies found in Phase II
-  Bore holes intersected massive sulphide
-  Other TEM anomalies
-  Other bore holes

Fig. III-1 Location map of Ore bodies, TEM anomalies and bore holes in Ghuzayn area

CHAPTER 2 RECOMMENDATIONS

Results of two years surveys show that the Central Batinah Coast area has a high potential for bearing massive sulphide deposits. As a continuation to the exploration program for the project, drilling and geophysical surveys are required in the areas of Ghuzayn, Doqal and Daris area as follows:

(1) Ghuzayn Area

- 1) Drilling survey is recommended to clarify the details of Northern and Western ore bodies found in this Phase II, along with TEM survey by using small loops(50m x 50m) to delineate in more detail the extension of bodies and to allocate drilling targets.
- 2) Drilling and TEM small loop surveys are recommended to investigate other anomalies detected by the TEM large loop survey carried out in this phase II.
- 3) TDIP survey is recommended around the area where TDIP was carried out in Phase I, in order to evaluate the total potential for mineralization in Ghuzayn area.

(2) Doqal Area

- 1) Drilling survey is recommended to be carried out to investigate the mineralization on the anomalies detected by TDIP and TEM surveys in this Phase.
- 2) Since TEM anomalies still continue towards north beyond the Phase II TEM survey area, it is necessary to conduct a TEM survey in northern part in order to delineate an accurate extension of anomaly zone. In addition, TEM survey is recommended to be carried out in the western part where IP anomaly is extended.
- 3) TDIP survey is recommended around the area where TDIP was carried out in Phase I, in order to evaluate the total potential for mineralization in Doqal area.

(3) Daris Area

- 1) Since the high metal factor zone detected in Phase I during the TDIP survey needs of further clarification, it is recommended to continue with TEM survey in selected locations defined by high metal factors detected in the central-western part of this area.

REFERENCES

- 1) BECHENNEC F., BEURRIER M., RABU D. and HUTIN G.(1986): Geological map of BARKA, -Sheet NF 40-3B, scale 1:100,000: explanatory notes.
- 2) BECHENNEC F., ROGER J., MRTOUR J.L., WYNS R. and CHEVREL S.(1992): Geological map of IBRI, -Sheet NF 40-02, scale 1:250,000: explanatory notes.
- 3) BECHENNEC F., ROGER J., MRTOUR J.L. and WYNS R.(1992): Geological map of SEEB, -Sheet NF 40-03, scale 1:250,000: explanatory notes.
- 4) BEURRIER M., BECHENNEC F., RABU D. and HUTIN G.(1986): Geological map of AS SUWAYQ, -Sheet NF 40-3A, scale 1:100,000: explanatory notes.
- 5) BEURRIER M., BECHENNEC F., RABU D. and HUTIN G.(1986): Geological map of RUSTAQ, -Sheet NF 40-3A, scale 1:100,000: explanatory notes.
- 6) BISHIMETAL EXPLORATION CO LTD.(1987): Report on a copper exploration programme in the northern part of the Oman mountains: Volume I: General
- 7) BISHIMETAL EXPLORATION CO LTD.(1991): Report on geologic and geophysical surveys in the TAWI RAKAH area, Sultanate of Oman
- 8) BISHIMETAL EXPLORATION CO LTD.(1992): Geophysical study in the prospects of Lasail west and Aarja in Sohar area and Hayl As Safil in Rakah area, Sultanate of Oman: Final Report
- 9) BRGM(1994): Mineral occurrences catalogue, BRGM, 119 p..
- 10) Cooper, N. J. and Swift, R.(1994): Application of TEM to Cyprus-type massive sulfide exploration in Cyprus, [Geophysics], vol.59, No.2, 202-214 p..
- 11) HADDADIN M.A., SULAIMAN Z.K. and AL-FORI S.S.(1983): The Ghuzayn copper-iron prospect, re-evaluation, Khaburah district, Oman. M.P.M., Department of Minerals, 28 p.
- 12) ISLES D.J. and WITHAM W.J.A.(1993): Explanatory notes on the solid geological interpretation of AS SUWAYQ 1:100,000 sheet NF40-3A, World Geoscience Corporation, 15 p..
- 13) ISLES D.J. and WITHAM W.J.A.(1993): Explanatory notes on the solid geological interpretation of BARKA 1:100,000 sheet NF40-3B, and part of NAKHL 1:100,000 sheet NF40-3E, World Geoscience Corporation, 13 p..
- 14) ISLES D.J. and WITHAM W.J.A.(1993): Explanatory notes on the solid geological interpretation of SIB 1:100,000 sheet NF40-3C, and part of FANJAY 1:100,000 sheet NF40-3F, World Geoscience Corporation, 11 p..
- 15) JEBRAK M., LETALENET J. and LESCUYER(1985): Detailed and semi-detailed exploration for copper and associated gold in the Daris, Mahab, Rakah, Ghuzayn, Wadi Andam, Washihi and Al Ajal Area, Interim report, BRGM, 52-57 p..
- 16) JICA and MMAJ(1990): Report on the mineral exploration in the Rakah area, Sultanate of Oman,

Bishimetal Exploration Co. Ltd.

- 17) LESCUYER J.L. and DEGAY E.(1986): Detailed and semi-detailed exploration for copper and associated gold in the DARIS, MAHAB, RAKAH, SHINAS, GHUZAYN, WADI ANDAM, WASHIHI and AL AJAI areas: Final report, BRGM, 125 p.. 4 appendices.
- 18) LESCUYER J.L., VACHETTE C. and BEURRIER M.(1989): Selection of zones for additional copper reserves between SHINAS and AL KHABURAH, northern Oman mountains: Final report, BRGM, 245 p..
- 19) O.C.M.C.(1994): Daris-part 5: Geological ore reserves at Daris 3A-5 as on 28 September 1994, Oman Mining Company, 10 p..
- 20) M.P.M.(1991): Summary of Cu prospects and recommendation for next programme M.P.M. of sultanate of Oman, 19 p..
- 21) M.P.M.(1995): GEOLOGY AND MINERAL WEALTH OF THE SULTANATE OF OMAN
- 22) RABU D., BECHENNEC F., BEURRIER M. and HUTIN G.(1986): Geological map of NAKHL, -Sheet NF 40-3E, scale 1:100,000: explanatory notes.
- 23) VILLEY M., BECHENNEC F., BEURRIER M., METOUR J. and RABU D.(1986): Geological map of YANQUL, -Sheet NF 40-2C, scale 1:100,000: explanatory notes.
- 24) Webster, S.(1995): Discussion on The application of TEM to Cyprus-type massive sulfide exploration in Cyprus, Geophysics, vol.60, No.5, 1 p..
- 25) World Geoscience Co.(1994): Report on ground geophysical surveys in the Sultanate of Oman, 5.4 Daris 3A-5 prospect, O.M.C.O., 15-21 p..

LIST OF FIGURES, TABLES AND APPENDICES

List of Figures

- Fig.1 Location map of the Central Batinah Coast area
- Fig.2 Location map of the survey areas
- Fig.I-3-1 Geologic map of the Central Batinah Coast area
- Fig.I-3-2 Schematic distribution of Samail Volcanic Rocks and mineralization in Sohar area
- Fig.I-4-1 IP plane map in Doqal area
- Fig.I-4-2 TEM response compiled map in Ghuzayn area
- Fig.I-4-3 Location map of Ore bodies, TEM anomalies and boreholes in Ghuzayn area
- Fig. II -1-1 Stratigraphic columnar section of survey area
- Fig. II -1-2 Schematic formation processes of massive sulphide deposits in Sohar
- Fig. II -1-3 Geologic map and mineral showing of Ghuzayn Gossan
- Fig. II -1-4 Geologic profile of Ghuzayn Gossan
- Fig. II -1-5 Location map of previous surveys in Daris prospect area
- Fig. II -1-6 Cross section of borehole site in Daris prospect area
- Fig. II -1-7 Panel diagram of Daris 3A5 deposits
- Fig. II -1-8 Mineral showing of Doqal area
- Fig. II -1-9 Mineral showing of Ghuzayn village north area
- Fig. II -1-10 Mineral showing of Fardah and Sanah area
- Fig. II -2-1 Dipole-dipole array and plotting procedure
- Fig. II -2-2 Waveform produced by the transmitter
- Fig. II -2-3 Sampling interval of the TDIP receiver
- Fig. II -2-4 IP line locations in Fardah area
- Fig. II -2-5 Apparent resistivity pseudo-sections in Fardah area
- Fig. II -2-6 Chargeability pseudo-sections in Fardah area
- Fig. II -2-7 Metal factor pseudo-sections in Fardah area
- Fig. II -2-8 IP plane map at $n=1$ in Fardah area
- Fig. II -2-9 IP plane map at $n=2$ in Fardah area
- Fig. II -2-10 IP plane map at $n=3$ in Fardah area
- Fig. II -2-11 IP plane map at $n=4$ in Fardah area
- Fig. II -2-12 Results of model simulation on Line 200E in Fardah area
- Fig. II -2-13 IP line locations in Sanah area
- Fig. II -2-14 Apparent resistivity pseudo-sections in Sanah area
- Fig. II -2-15 Chargeability pseudo-sections in Sanah area

- Fig. II -2-16 Metal factor pseudo-sections in Sanah area
- Fig. II -2-17 IP plane map at n=1 in Sanah area
- Fig. II -2-18 IP plane map at n=2 in Sanah area
- Fig. II -2-19 IP plane map at n=3 in Sanah area
- Fig. II -2-20 IP plane map at n=4 in Sanah area
- Fig. II -2-2 Results of model simulation on Line 000E in Sanah area
- Fig. II -2-22 IP line locations in Ghuzayn north area
- Fig. II -2-23 Apparent resistivity pseudo-sections in Ghuzayn north area
- Fig. II -2-24 Chargeability pseudo-sections in Ghuzayn north area
- Fig. II -2-25 Metal factor pseudo-sections in Ghuzayn north area
- Fig. II -2-26 IP plane map at n=1 in Ghuzayn north area
- Fig. II -2-27 IP plane map at n=2 in Ghuzayn north area
- Fig. II -2-28 IP plane map at n=3 in Ghuzayn north area
- Fig. II -2-29 IP plane map at n=4 in Ghuzayn north area
- Fig. II -2-30 Results of model simulation on Line 000N in Ghuzayn North area
- Fig. II -2-31 IP line locations in Doqal area
- Fig. II -2-32 Apparent resistivity pseudo-sections in Doqal area
- Fig. II -2-33 Chargeability pseudo-sections in Doqal area
- Fig. II -2-34 Metal factor pseudo-sections in Doqal area
- Fig. II -2-35 IP plane map at n=1 in Doqal area
- Fig. II -2-36 IP plane map at n=2 in Doqal area
- Fig. II -2-37 IP plane map at n=3 in Doqal area
- Fig. II -2-38 IP plane map at n=4 in Doqal area
- Fig. II -2-39 Results of model simulation on Line 400N in Doqal area
- Fig. II -2-40 Results of model simulation on Line 200N in Doqal area
- Fig. II -2-41 Results of model simulation on Line 000N in Doqal area
- Fig. II -2-42 Results of model simulation on Line 200S in Doqal area
- Fig. II -3-1 Schematic TEM survey configuration
- Fig. II -3-2 Example of TEM decay curve
- Fig. II -3-3 TEM decay difference
- Fig. II -3-4(1) Contour plot of secondary magnetic response
- Fig. II -3-4(2) Contour plot of secondary magnetic response
- Fig. II -3-5(1) Contour plot of magnetic difference
- Fig. II -3-5(2) Contour plot of magnetic difference
- Fig. II -3-6 Ghuzayn survey site showing observation points

- Fig. II -3-7(1) TEM response plane maps of Loop1 in Ghuzayn area
- Fig. II -3-7(2) TEM response plane maps of Loop1 in Ghuzayn area
- Fig. II -3-8(1) TEM response plane maps of Loop2 in Ghuzayn area
- Fig. II -3-8(2) TEM response plane maps of Loop2 in Ghuzayn area
- Fig. II -3-9(1) TEM response plane maps of Loop3 in Ghuzayn area
- Fig. II -3-9(2) TEM response plane maps of Loop3 in Ghuzayn area
- Fig. II -3-10(1) TEM response plane maps of Loop4 in Ghuzayn area
- Fig. II -3-10(2) TEM response plane maps of Loop4 in Ghuzayn area
- Fig. II -3-11(1) TEM response plane maps of Loop5 in Ghuzayn area
- Fig. II -3-11(2) TEM response plane maps of Loop5 in Ghuzayn area
- Fig. II -3-12(1) TEM response plane maps of Loop6 in Ghuzayn area
- Fig. II -3-12(2) TEM response plane maps of Loop6 in Ghuzayn area
- Fig. II -3-13 TEM response compile maps in Ghuzayn area
- Fig. II -3-14 Daris North survey site showing observation points
- Fig. II -3-15(1) TEM response plane maps of Loop1 in Daris North area
- Fig. II -3-15(2) TEM response plane maps of Loop1 in Daris North area
- Fig. II -3-16(1) TEM response plane maps of Loop2 in Daris North area
- Fig. II -3-16(2) TEM response plane maps of Loop2 in Daris North area
- Fig. II -3-17(1) TEM response plane maps of Loop3 in Daris North area
- Fig. II -3-17(2) TEM response plane maps of Loop3 in Daris North area
- Fig. II -3-18 TEM response compile maps in Daris North area
- Fig. II -3-19 Fardah survey site showing observation points
- Fig. II -3-20(1) TEM response plane maps of Loop1 in Fardah area
- Fig. II -3-20(2) TEM response plane maps of Loop1 in Fardah area
- Fig. II -3-21 Sanah survey site showing observation points
- Fig. II -3-22(1) TEM response plane maps of Loop1 in Sanah area
- Fig. II -3-22(2) TEM response plane maps of Loop1 in Sanah area
- Fig. II -3-23(1) TEM response plane maps of Loop2 in Sanah area
- Fig. II -3-23(2) TEM response plane maps of Loop1 in Sanah area
- Fig. II -3-24 Doqal survey site showing observation points
- Fig. II -3-25(1) TEM response plane maps of Loop1 in Doqal area
- Fig. II -3-25(2) TEM response plane maps of Loop1 in Doqal area
- Fig. II -3-26(1) TEM response plane maps of Loop2 in Doqal area
- Fig. II -3-26(2) TEM response plane maps of Loop2 in Doqal area
- Fig. II -4-1 Location map of bore holes in Ghuzayn area

- Fig. II-4-2 Location map of bore holes in Daris area
- Fig. II-4-3 Location map of bore holes in Daris 3A5 area
- Fig. II-4-4 Location map of bore holes in Fardah area
- Fig. II-4-5 Cross section of borehole site in the northern body of Ghuzayn deposit
- Fig. II-4-6 Cross section of borehole site in the western body of Ghuzayn deposit
- Fig. II-4-7 IP pseudo-section around northern body of Ghuzayn deposit
- Fig. II-4-8 IP pseudo-section around western body of Ghuzayn deposit
- Fig. II-4-9 Schematic model of Daris and Rakah deposits
- Fig. II-4-10 Schematic model of massive sulphide deposit in Central Batinah Coast
- Fig. II-4-11 IP pseudo-section around bore holes in Daris area
- Fig. II-4-12 IP pseudo-section around bore holes in Daris 3A5 area
- Fig. II-4-13 IP pseudo-section around bore holes in Daris north area
- Fig. II-4-14 IP pseudo-section around bore holes in Fardah area
- Fig. II-5-1 Flow chart for massive sulfide exploration
- Fig. II-5-2(1) IP results plane map near Aarja and Bayda deposits
- Fig. II-5-2(2) IP results plane map near Aarja and Bayda deposits
- Fig. II-5-3 TEM response plane map in Bayda deposit
- Fig. II-5-4 IP Results plane map in Ghuzayn gossan area
- Fig. II-5-5 TEM anomaly comparison map with 50m and 600m loop
- Fig. III-1 Location map of Ore bodies, TEM anomalies and bore holes in Ghuzayn area

List of Tables

- Table I-1-1 Content and amount of work in Phase II
- Table I-1-2 Laboratory work in Phase II
- Table I-4-1 Summary of results on drilling survey in Ghuzayn area
- Table II-1-1 Comparison of pillow lavas in Samail ophiolite
- Table II-2-1 Survey Amounts of TDIP
- Table II-2-2 Specifications of TDIP survey instruments
- Table II-2-3 Resistivity and chargeability of core samples
- Table II-3-1 Survey amounts of TEM
- Table II-3-2 Channel times after switch off
- Table II-3-3 Specifications of TEM survey instruments
- Table II-3-4 Depth estimation in survey area

- Table II -4-1 Drilling survey conducted in Phase II
- Table II -4-2 Description of thin sections of drilling core
- Table II -4-3 Description of polished section of drilling core
- Table II -4-4 Results of X-ray diffraction analyses of drilling core
- Table II -4-5 Summary of results on drilling survey in Ghuzayn area

List of Appendices

- Appendix 1 Drilling equipments and consumed materials
- Appendix 2 Generalized drilling results and Progress record of drilling
- Appendix 3 Drilling logs
- Appendix 4 Assay results of drilling core
- Appendix 5 Photographs of ore polished sections

APPENDICES

Appendix 1

Drilling equipments and consumed materials

Drilling Equipment

	Rig-1	Rig-2	Rig-3	Rig-4
Model	RAMROD-II	VOL-180	N-18(F4L)	N-18(f5L)
Maker	Joy Manufacturing Co. USA	Voltas Ltd. India	Acker Drill Co. USA	Acker Drill Co. USA
Mounting	Truck mounted 4WD	Truck mounted 4WD	Skid Mounted	Skid Mounted
Drilling capacity with NX size wire Line coring	450 m	650 m	400 m	600 m
Angle hole drilling capacity	Upto 60 deg.	Vertical only	Upto 60 deg.	Upto 60 deg.
Circulation pump	35 GPM 800 PSI	37 GPM 1000 PSI	35 GPM 800 PSI	37 GPM 1000 PSI

Consumed material

Hole No.	MJOB-G1	MJOB-G2	MJOB-G3	MJOB-G4	MJOB-G5	MJOB-G6	MJOB-G7	MJOB-G8	MJOB-G9
Bit: NW	1	1	1	1	1	1	1	1	1
Bit: NX	1	1	1	1	1	3	2	1	1
Bit: BX			1						
Light Oil (l)	25	35	40	40	30	30	30	15	15
Mud (kg)	185	260	290	265	210	230	210	120	115
Cement (kg)	50	-	75	125	75	100	150	200	200

Hole No.	MJOB-G10	MJOB-G11	MJOB-G12	MJOB-G13	MJOB-G14	MJOB-G15	MJOB-G16	MJOB-G17	MJOB-D1
Bit: NW	1	1	1	1	1	1	1	1	1
Bit: NX	1	1	1	2	1	1	1	2	1
Bit: BX									
Light Oil (l)	15	15	15	15	20	20	20	25	25
Mud (kg)	105	105	115	115	155	165	130	190	165
Cement (kg)	-	100	75	150	100	150	175	125	-

Hole No.	MJOB-D2	MJOB-D3	MJOB-D4	MJOB-R1	MJOB-A1	MJOB-A2	MJOB-F1	MJOB-F2
Bit: NW	1	1	1	1	1	1	1	1
Bit: NX	1	1	1	1	1	2	1	1
Bit: BX						1		
Light Oil (l)	25	15	30	30	30	20	20	20
Mud (kg)	140	105	215	125	200	480	145	150
Cement (kg)	-	-	-	-	500	200	-	-

Appendix 2

Generalized drilling results and progress record of drilling



Generalized drilling results

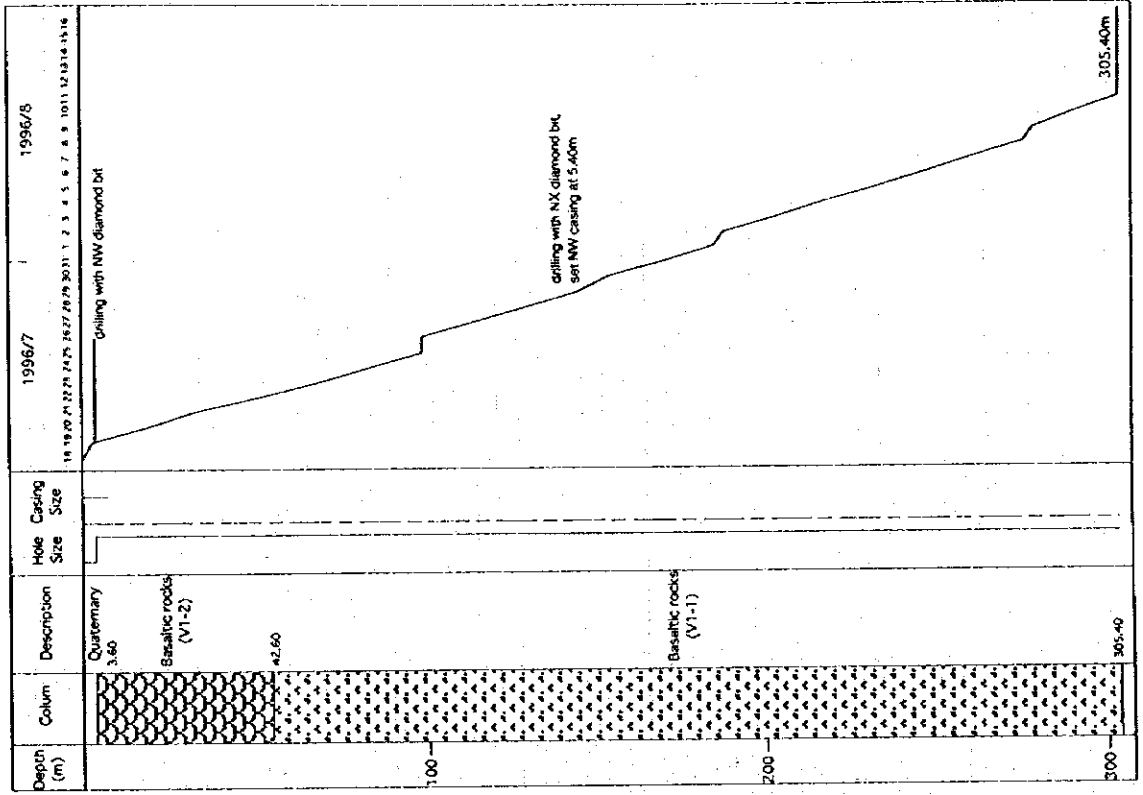
Hole No.		MJOB-G1	MJOB-G2	MJOB-G3	MJOB-G4	MJOB-G5	MJOB-G6	MJOB-G7
Drilling Period	Preparation Days (A)	7/17 to 7/20 4	7/16 to 7/18 3	8/8 1	8/12 1	9/10 1	9/18 1	10/11 1
	Drilling Days (B)	7/21 to 8/6 17	7/19 to 8/11 23	8/9 to 9/7 30	8/13 to 9/16 35	9/11 to 9/29 19	9/19 to 10/9 21	10/12 to 10/30 18.5
	Removing Days (C)	8/7 1	8/12 1	9/8 to 9/9 2	9/17 1	9/30 1	10/10 1	10/30-10/31 1.5
	Total days (D)	22	27	33	37	21	23	21
Depth	Planned depth (E)	186m	305m	300m	300m	300m	300m	300m
	Drilled depth (F)	186.50m	305.40m	300.40m	300.50m	300.20m	300.30m	300.15m
Recovery	Overburden (G)	3.40m	3.60m	6.10m	5.30m	10.10m	11.80m	11.00m
	Core length (H)	183.25m	304.40m	296.05m	295.80m	294.95m	291.05m	294.05m
	Recovery (H/F)	98%	100%	99%	98%	98%	97%	98%
Casing	NW casing	3.40m	5.40m	3.40m	5.30m	3.40m	3.40m	3.40m
	NX casing	-	-	257.10m	295.80m	-	-	-
Rate	meter /day (F/B)	10.97m	13.28m	10.01m	8.59m	15.80m	14.30m	16.22m
	meter/ total day (F/D)	8.48m	11.31m	9.10m	8.12m	14.30m	13.06m	14.29m

Hole No.		MJOB-G8	MJOB-G9	MJOB-G10	MJOB-G11	MJOB-G12	MJOB-G13	MJOB-G14
Drilling Period	Preparation Days (A)	10/1 1	9/30 to 10/1 2	10/13 1	10/12 1	10/22 1	10/23 1	11/2 1
	Drilling Days (B)	10/2 to 10/11 10	10/2 to 10/11 9.5	10/14 to 10/22 8.5	10/13 to 10/21 9	10/23 to 11/2 10.5	10/24 to 11/3 10.5	11/3 to 11/26 24.5
	Removing Days (C)	10/12 1	10/11 0.5	10/22 0.5	10/22 1	11/2 0.5	11/3 0.5	11/26 to 11/27 1.5
	Total days (D)	12	12	10	11	12	12	27
Depth	Planned depth (E)	200m	200m	200m	200m	200m	200m	250m
	Drilled depth (F)	200.25m	200.20m	200.10m	200.20m	200.30m	200.10m	250.10m
Recovery	Overburden (G)	4.90m	7.35m	5.80m	4.60m	4.80m	4.70m	2.80m
	Core length (H)	194.75m	196.00m	197.20m	196.00m	196.65m	196.75m	240.55m
	Recovery (H/F)	97%	98%	99%	98%	98%	98%	96%
Casing	NW casing	3.40m	3.40m	3.40m	3.40m	3.40m	5.40m	3.40m
	NX casing	-	-	-	-	-	-	-
Rate	meter /day (F/B)	20.03m	21.07m	23.54m	22.24m	19.08m	19.06m	10.21m
	meter/ total day (F/D)	16.69m	16.68m	20.01m	18.20m	16.69m	16.68m	9.26m

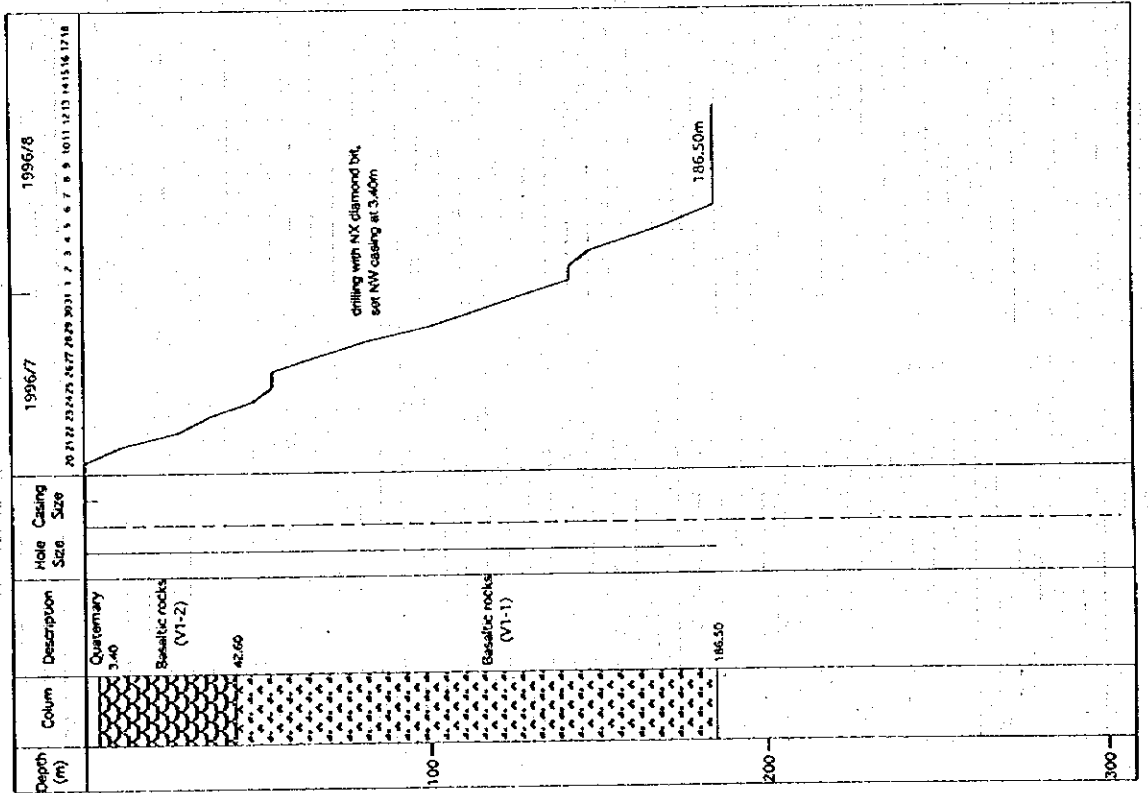
Hole No.	MJOB-G15	MJOB-G16	MJOB-G17	MJOB-D1	MJOB-D2	MJOB-D3	MJOB-D4	
Drilling Prod	Preparation Days (A)	11/4 1	11/20 1	11/20 1	7/14 to 7/15 2	8/1 0.5	8/13 0.5	10/22 1
	Drilling Days (B)	11/5 to 11/18 14	11/21 to 12/5 15	11/21 to 12/10 19.5	7/16 to 7/30 15	8/1 to 8/12 11.5	8/14 to 8/21 8	10/23 to 11/5 14
	Removing Days (C)	11/19 1	12/6 to 12/7 2	12/10 to 12/11 1.5	7/31 1	8/13 0.5	8/22 to 8/23 2	11/6 1
	Total days (D)	16	18	22	18	12.5	10.5	16
Depth	Planned depth (E)	250m	200m	250m	220m	250m	150m	300m
	Drilled depth (F)	250.10m	201.85m	250.25m	220.15m	251.00m	150.35m	300.35m
Recovery	Overburden (G)	3.50m	4.80m	6.70m	3.70m	4.95m	3.50m	4.50m
	Core length (H)	247.40m	196.90m	241.30m	215.40m	248.70m	148.45m	297.95m
	Recovery (H/F)	99%	98%	97%	98%	99%	99%	99%
Casing	NW casing	3.40m	3.40m	3.40m	13.50m	19.40m	13.50m	38.00m
	NX casing	-	-	-	-	-	-	-
Rate	meter /day (F/B)	17.86m	13.46m	12.83m	14.68m	21.83m	18.79m	21.45m
	meter/ total day (F/D)	15.63m	11.21m	11.38m	12.23m	20.08m	14.32m	18.77m

Hole No.	MJOB-R1	MJOB-A1	MJOB-A2	MJOB-F1	MJOB-F2	
Drilling Prod	Preparation Days (A)	10/23 1	8/24 1	9/13 1	11/8 1	11/5 1
	Drilling Days (B)	10/24 to 11/3 11	8/25 to 9/11 18	9/14 to 10/8 25	11/9 to 11/21 12.5	11/6 to 11/18 13
	Removing Days (C)	11/4 1	9/12 1	10/9 to 10/10 2	11/21 to 11/22 1.5	11/19 1
	Total days (D)	13	20	28	15	15
Depth	Planned depth (E)	200m	250m	227m	250m	200m
	Drilled depth (F)	200.15m	251.00m	227.00m	250.65m	200.20m
Recovery	Overburden (G)	3.60m	2.60m	14.00m	0.00m	0.00m
	Core length (H)	195.35m	241.00m	220.75m	249.55m	196.00m
	Recovery (H/F)	98%	96%	97%	100%	98%
Casing	NW casing	61.25m	3.40m	3.40m	3.80m	6.40m
	NX casing	-	-	220.75m	-	-
Rate	meter /day (F/B)	18.20m	13.94m	9.08m	20.05m	15.40m
	meter/ total day (F/D)	15.40m	12.55m	8.11m	16.71m	13.35m

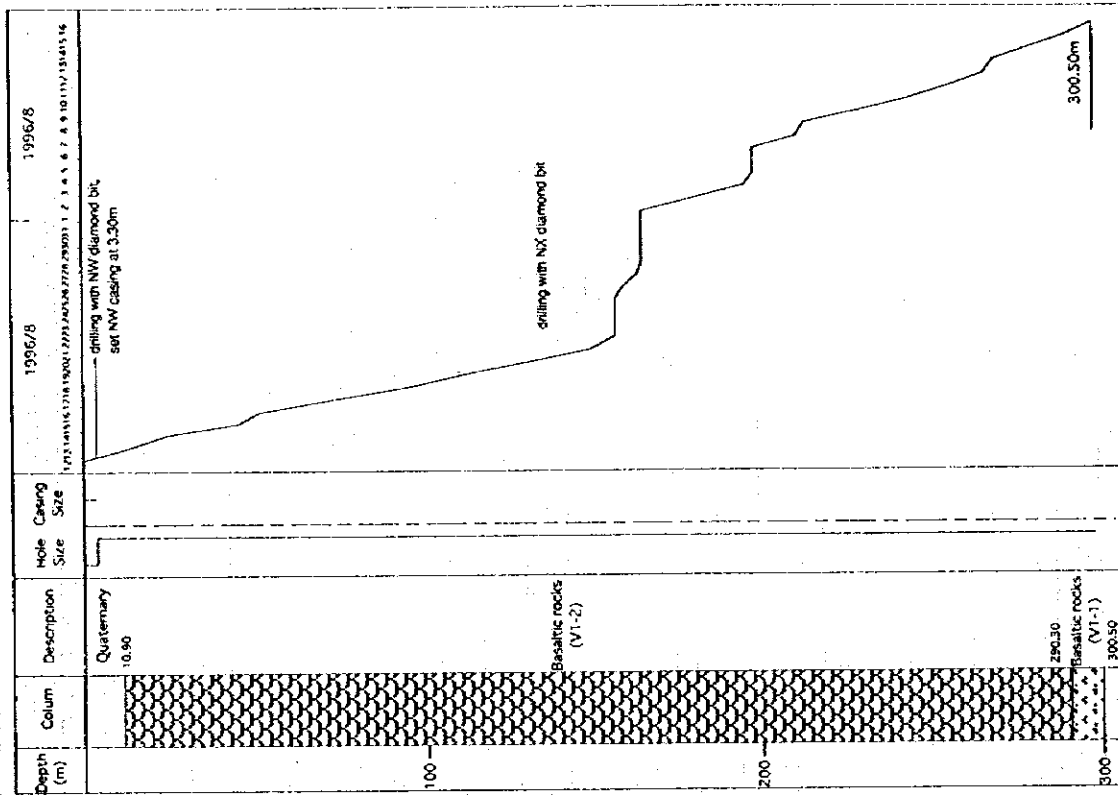
MJOB-G2



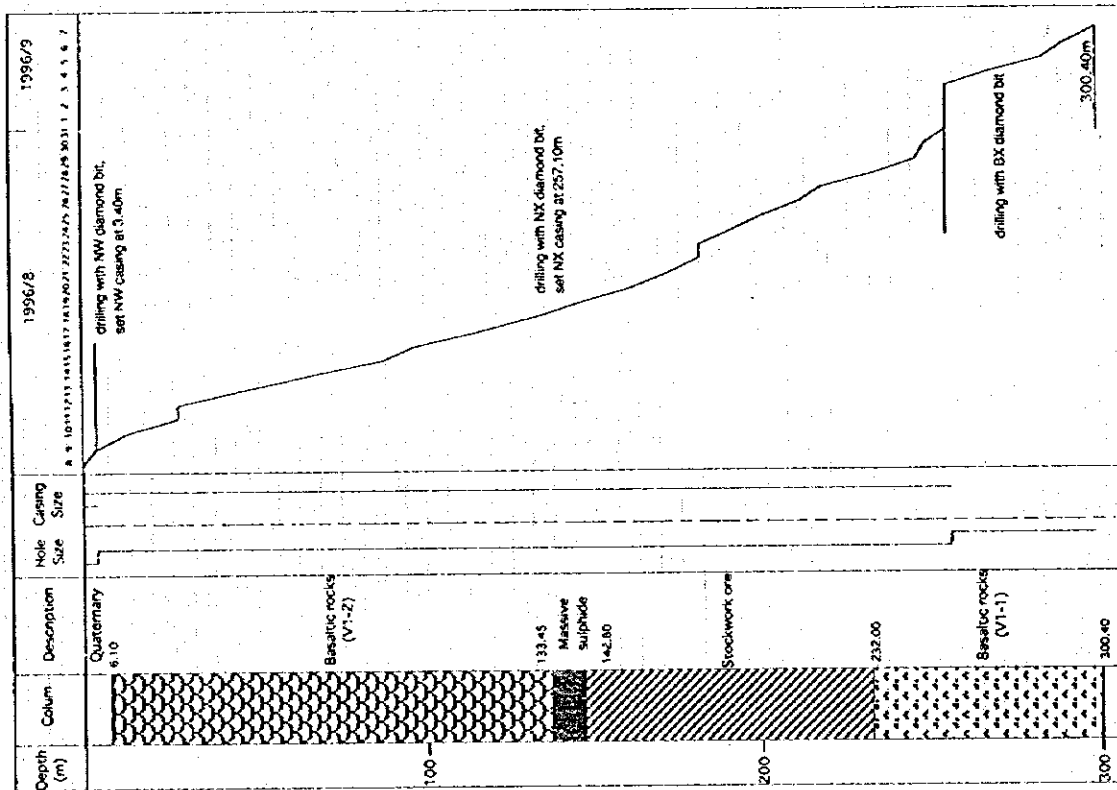
MJOB-G1



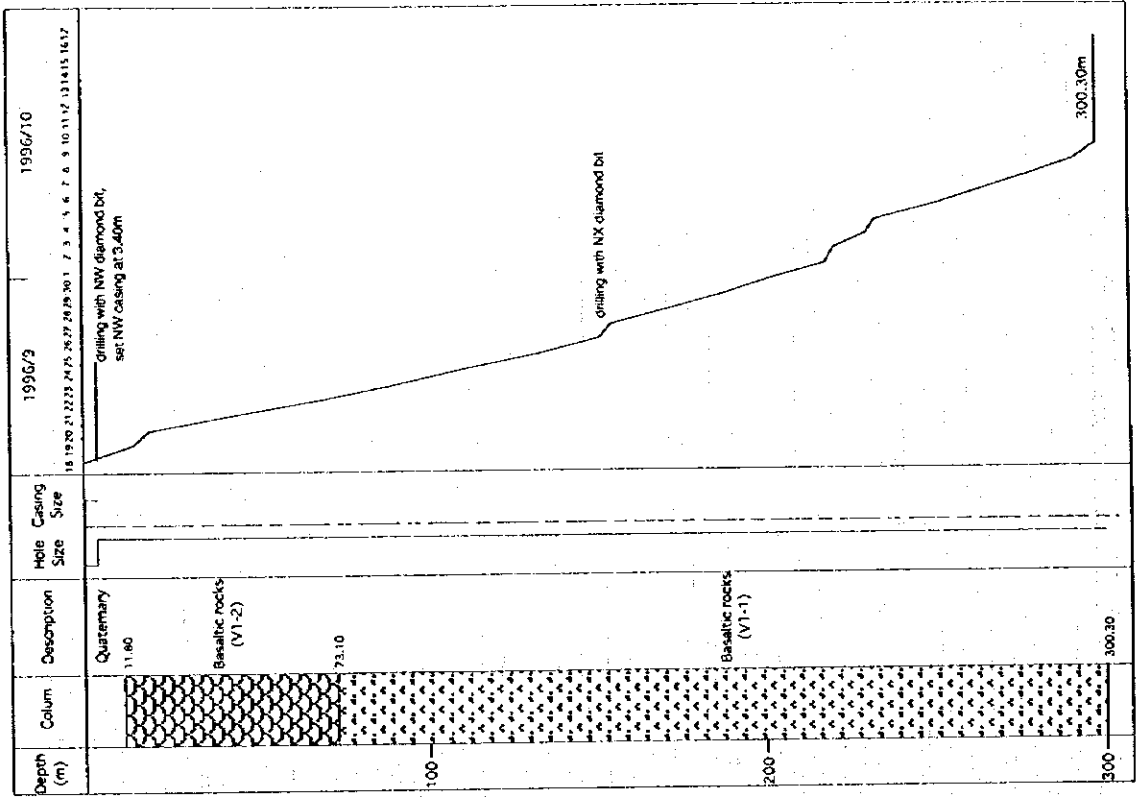
MJOB-G4



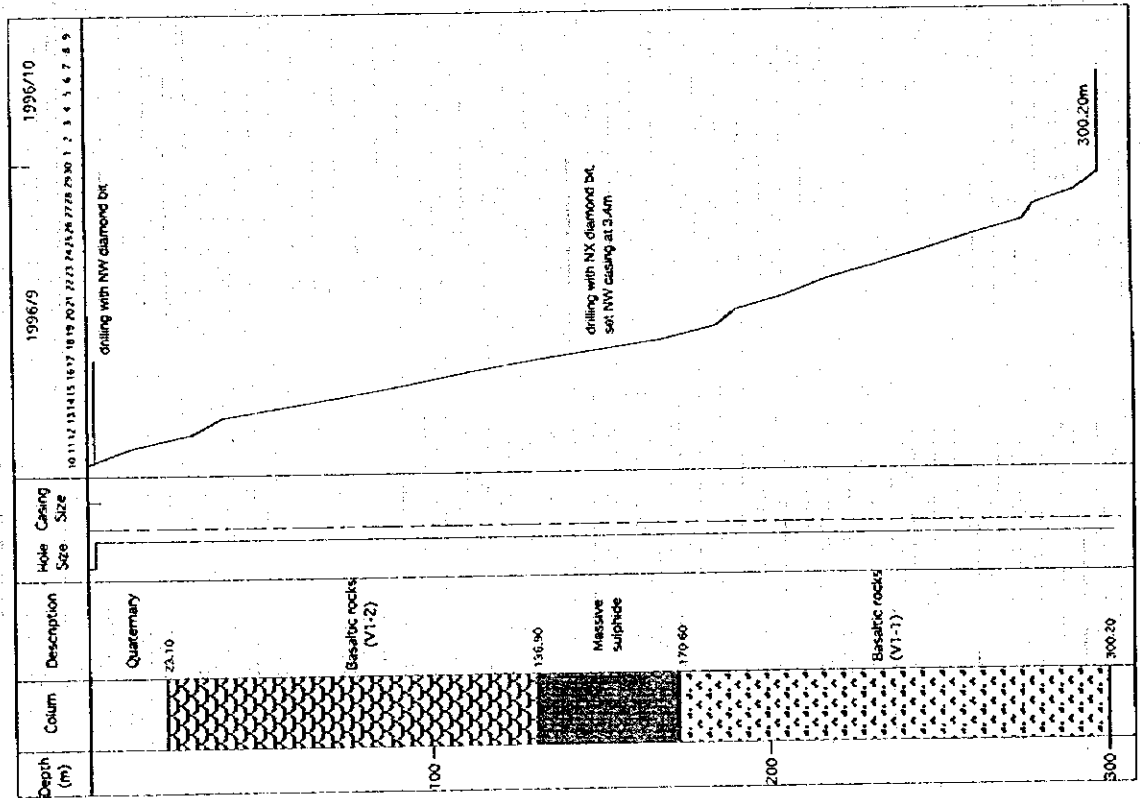
MJOB-G3



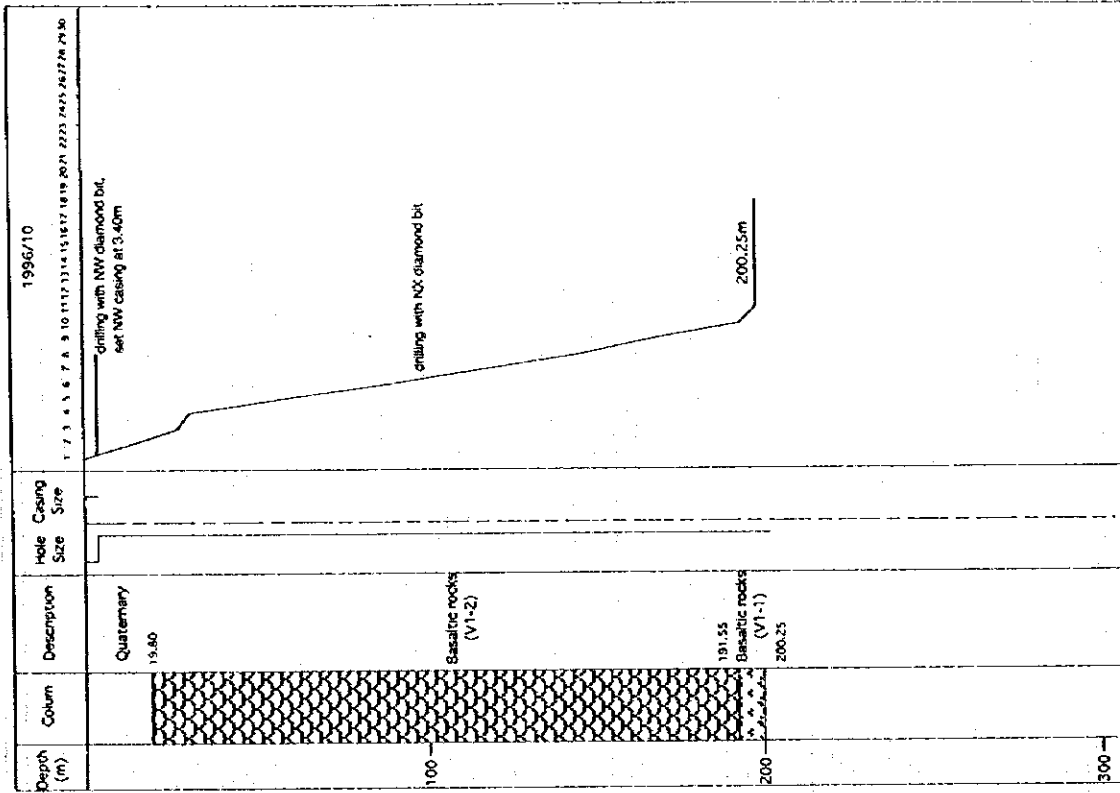
MJOB-G6



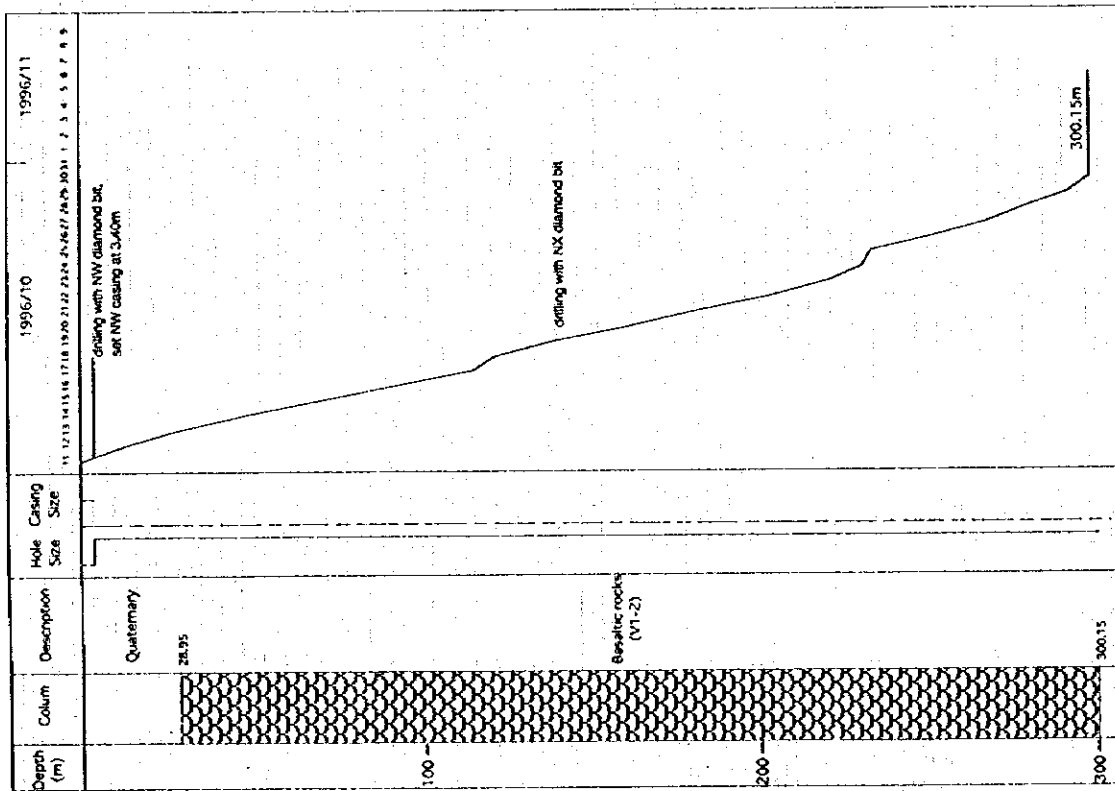
MJOB-G5



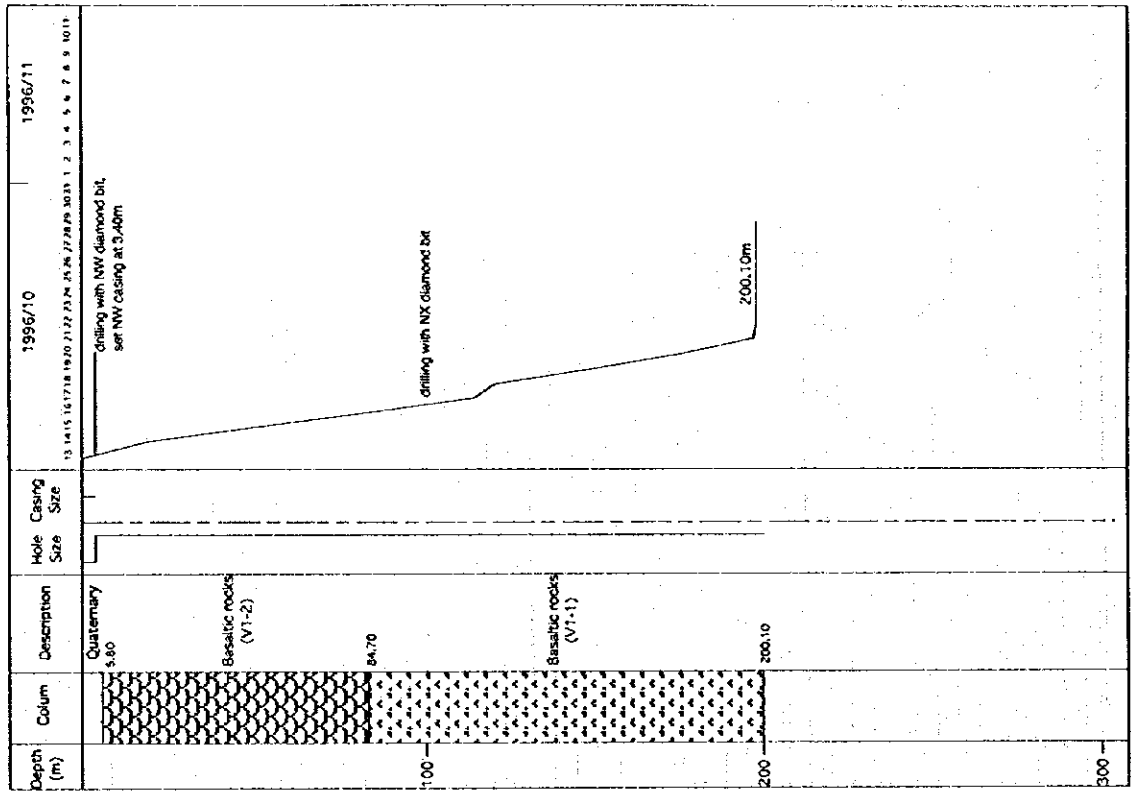
MJOB-G8



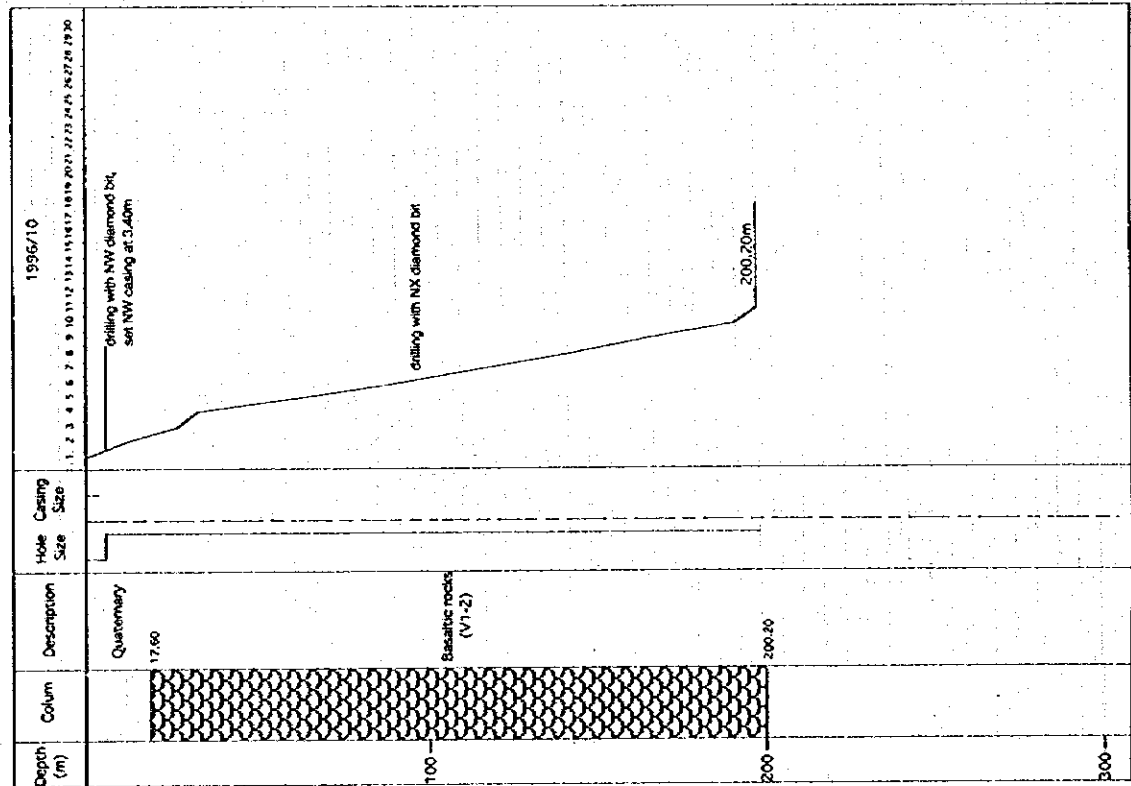
MJOB-G7



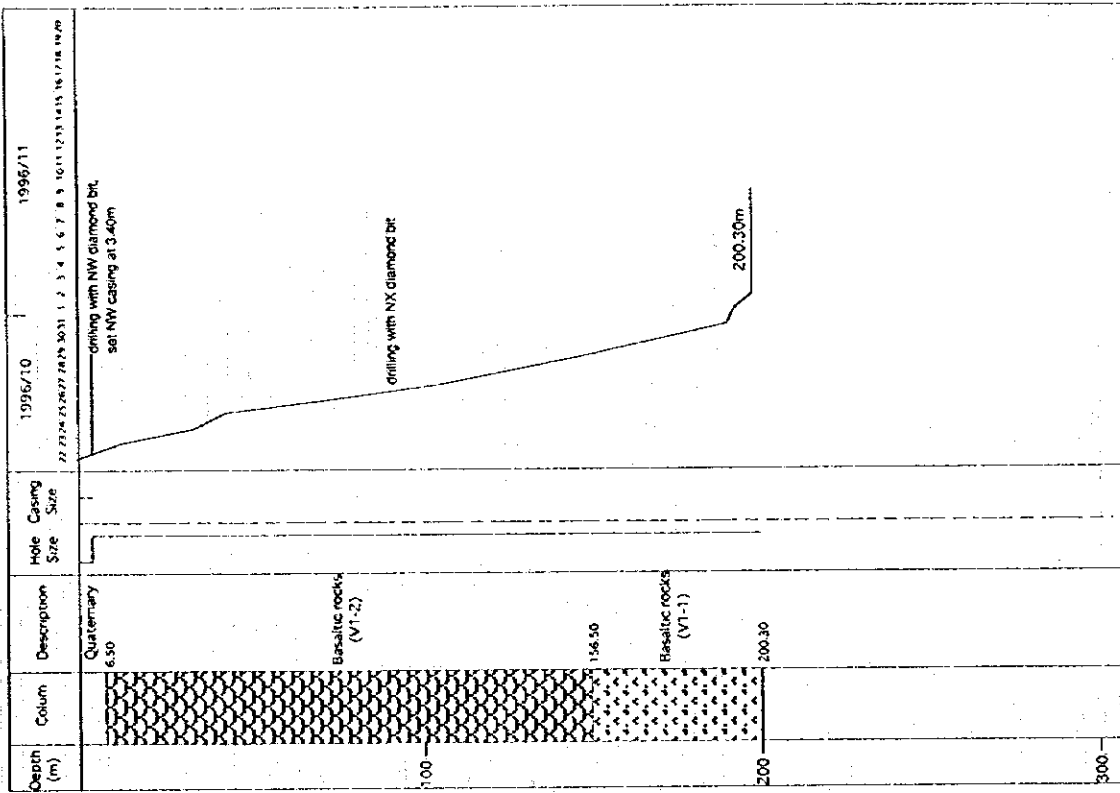
MJOB-G10



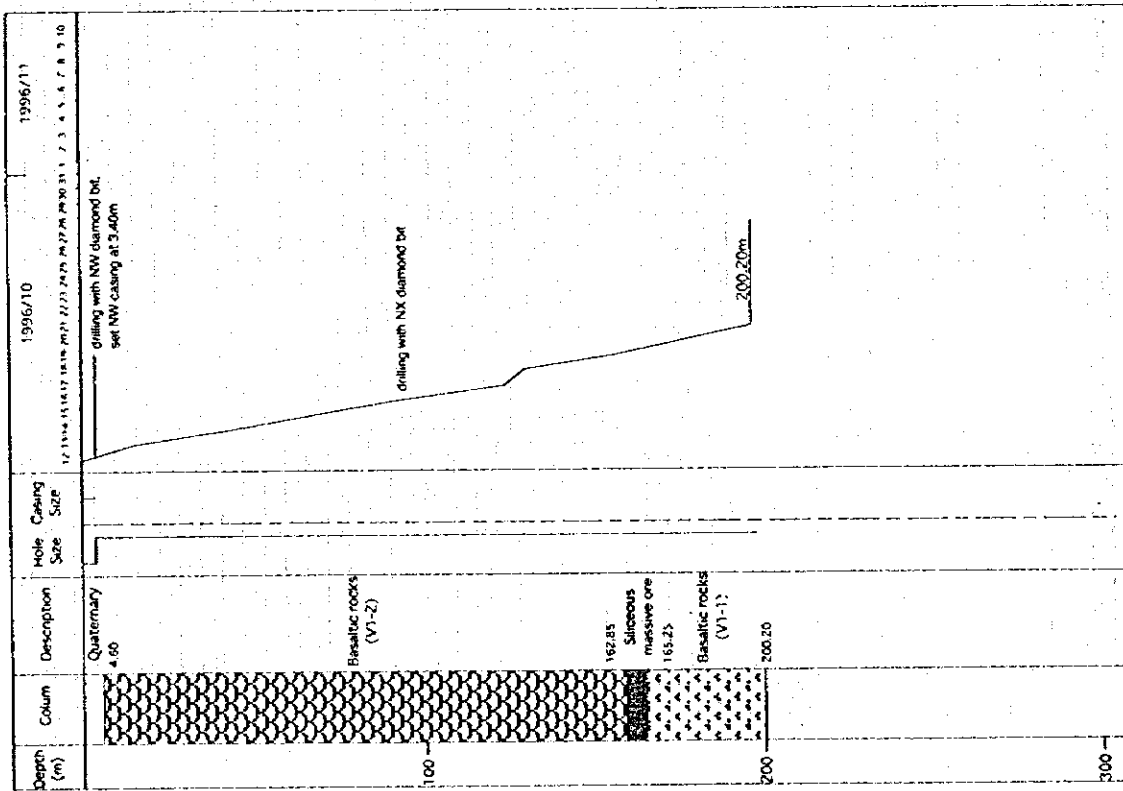
MJOB-G9



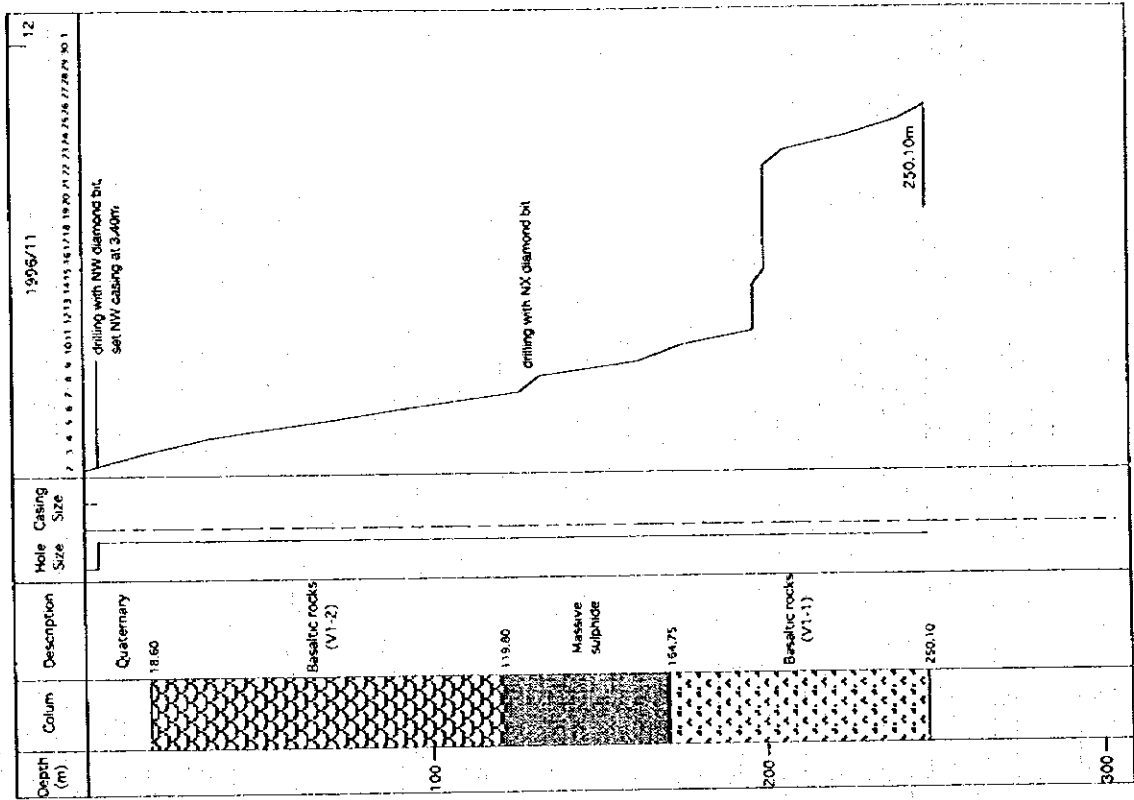
MJOB-G12



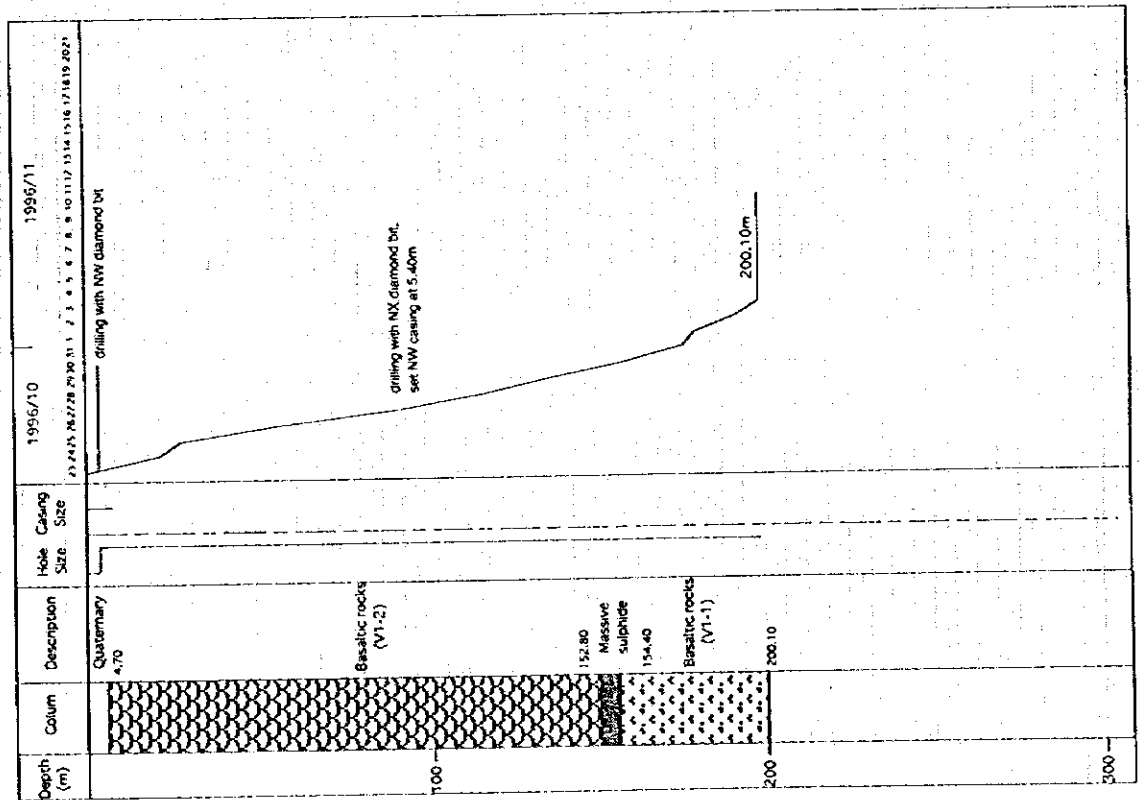
MJOB-G11



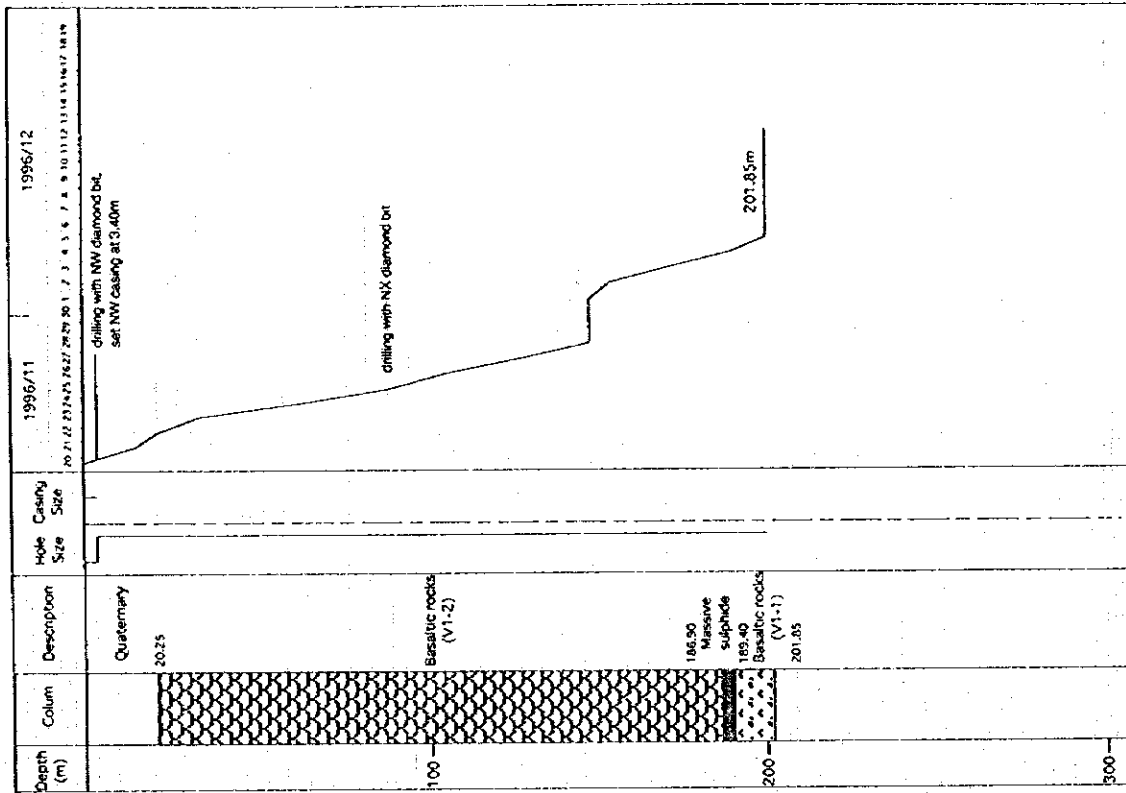
MJOB-G14



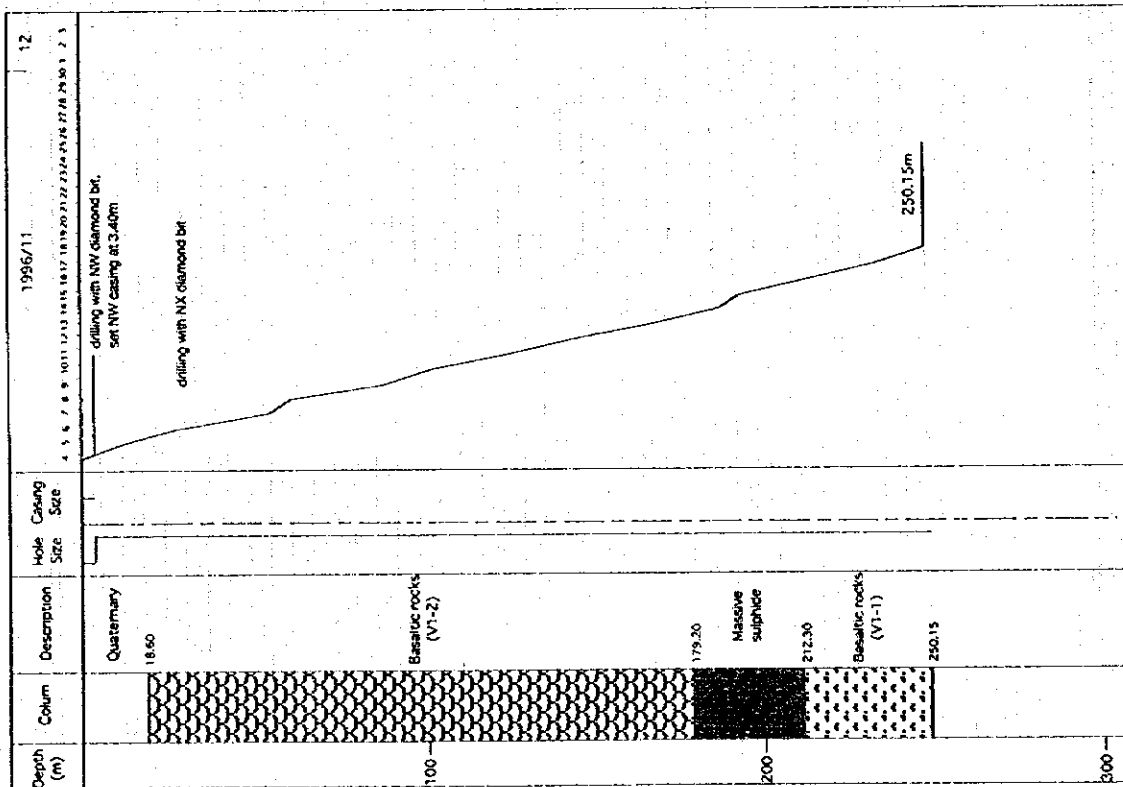
MJOB-G13



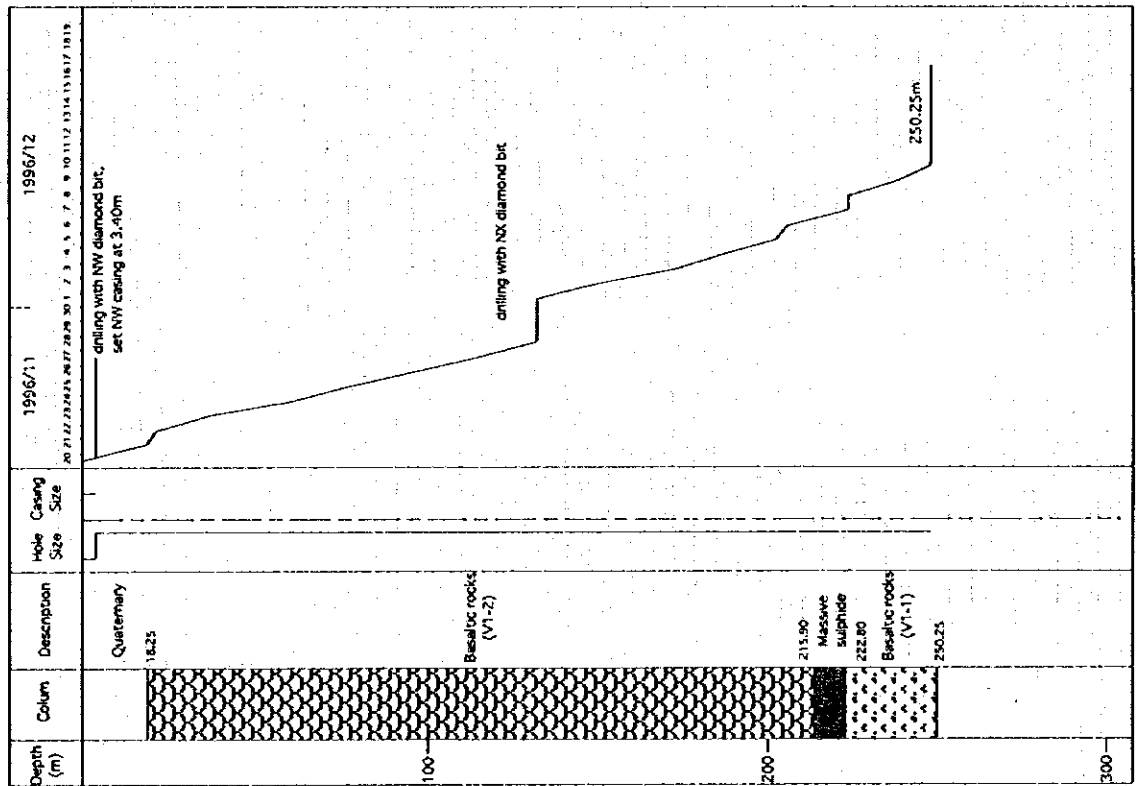
MJOB-G16



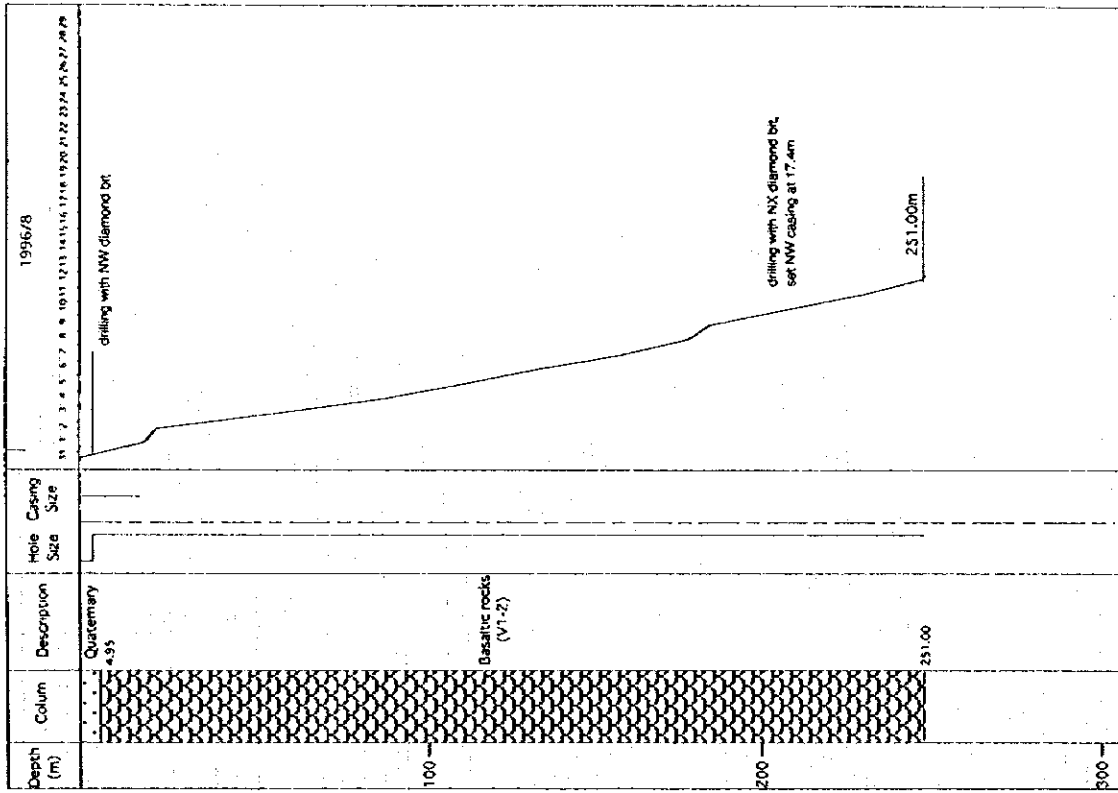
MJOB-G15



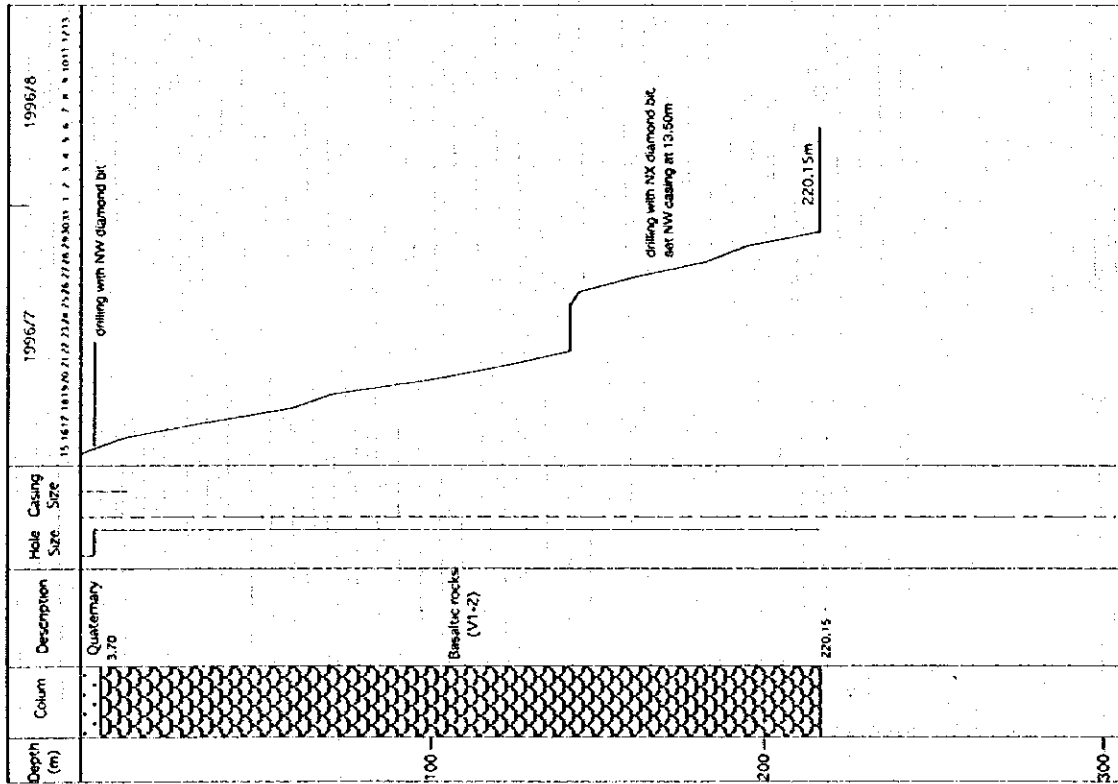
MJOB-G17



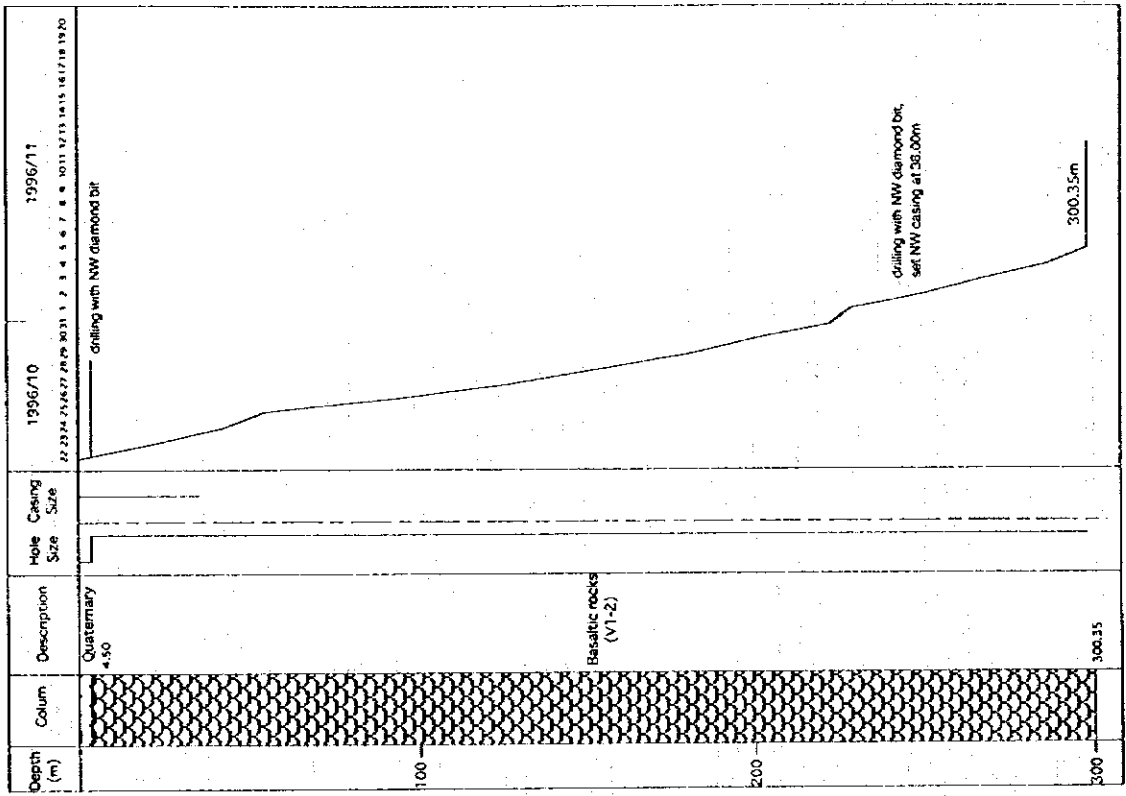
MJOB-D2



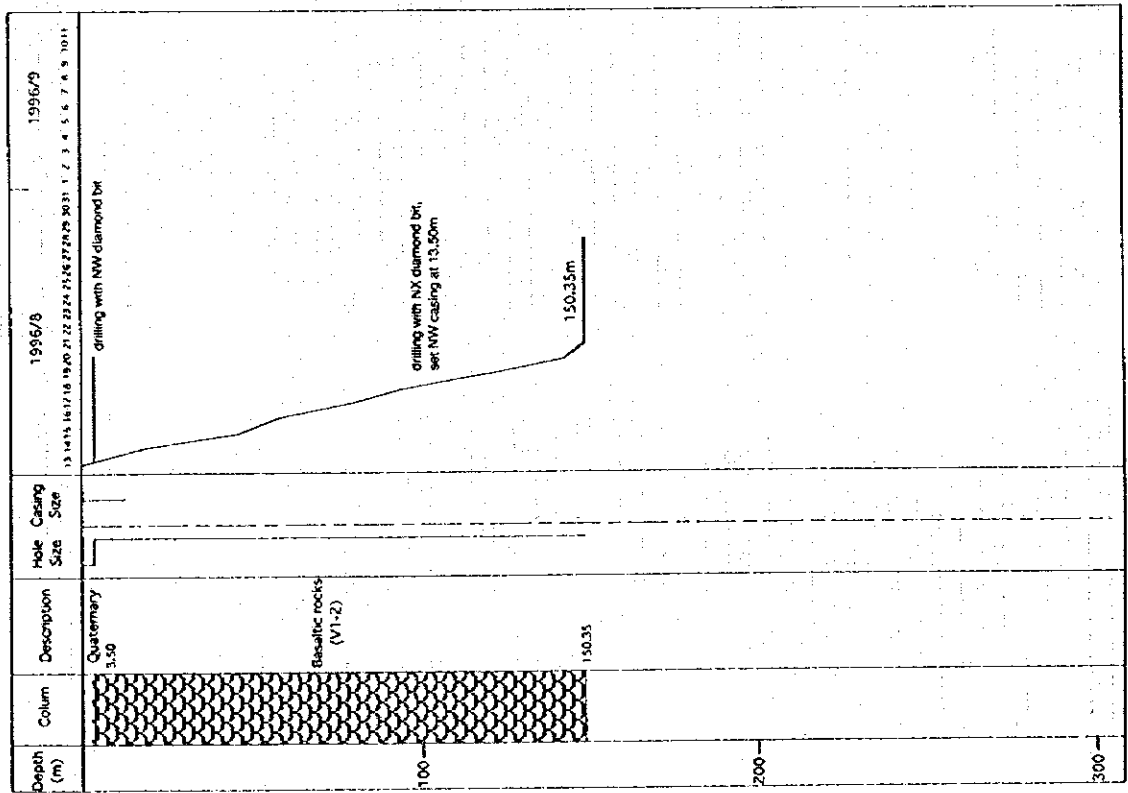
MJOB-D1



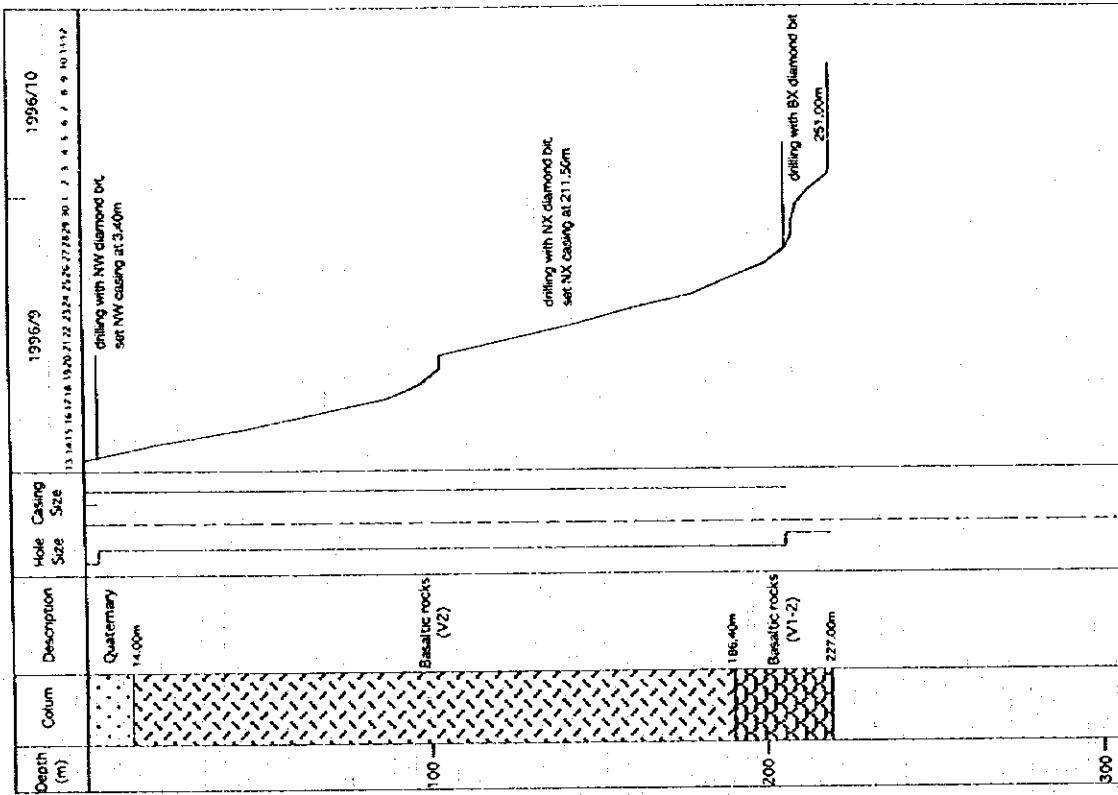
MJOB-D4



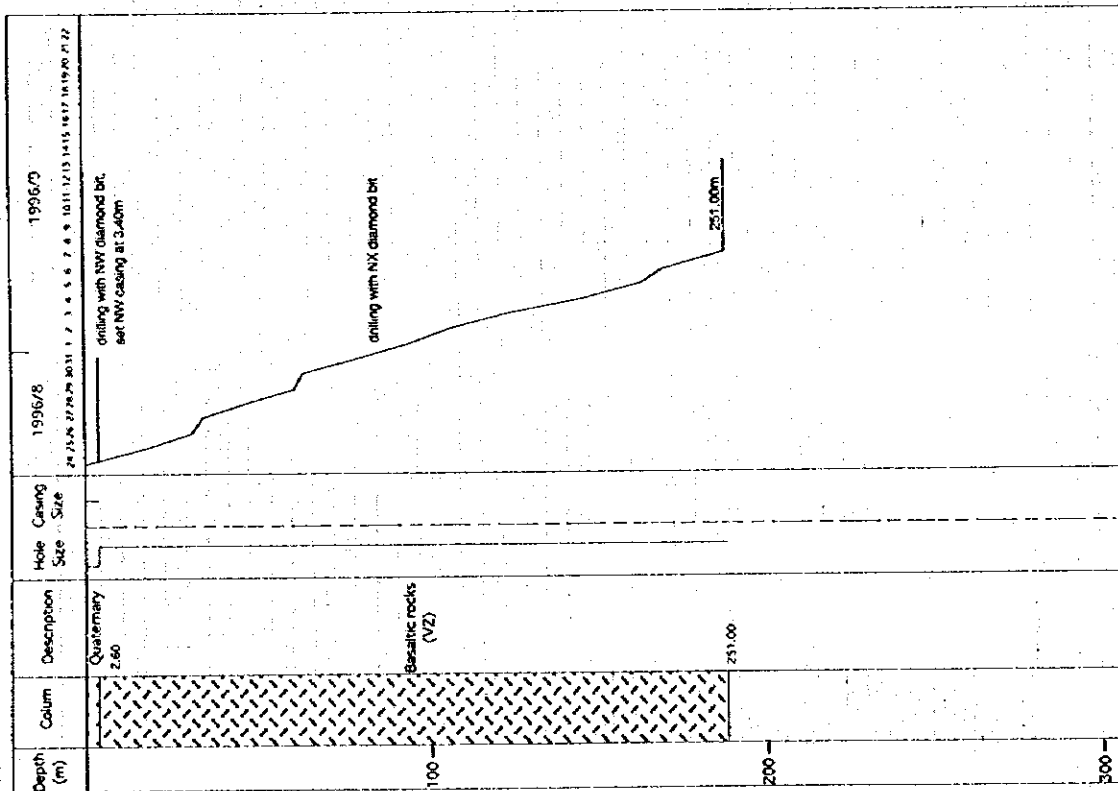
MJOB-D3



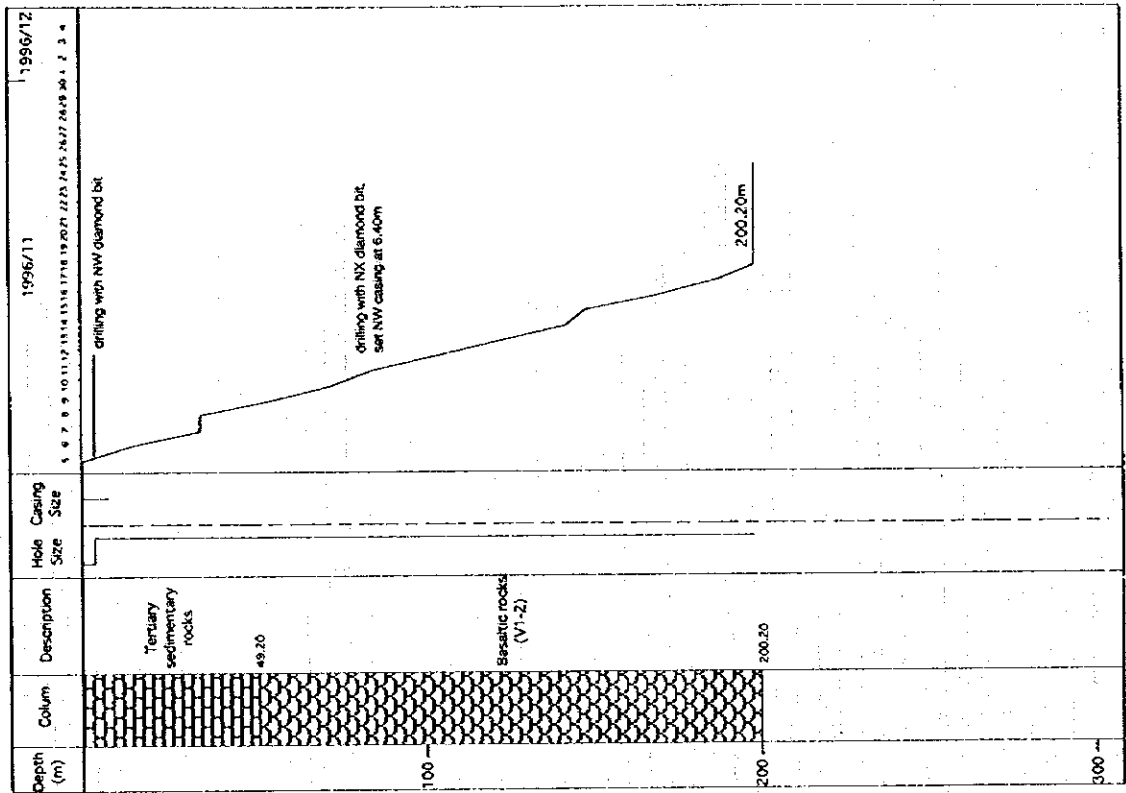
MJOB-A2



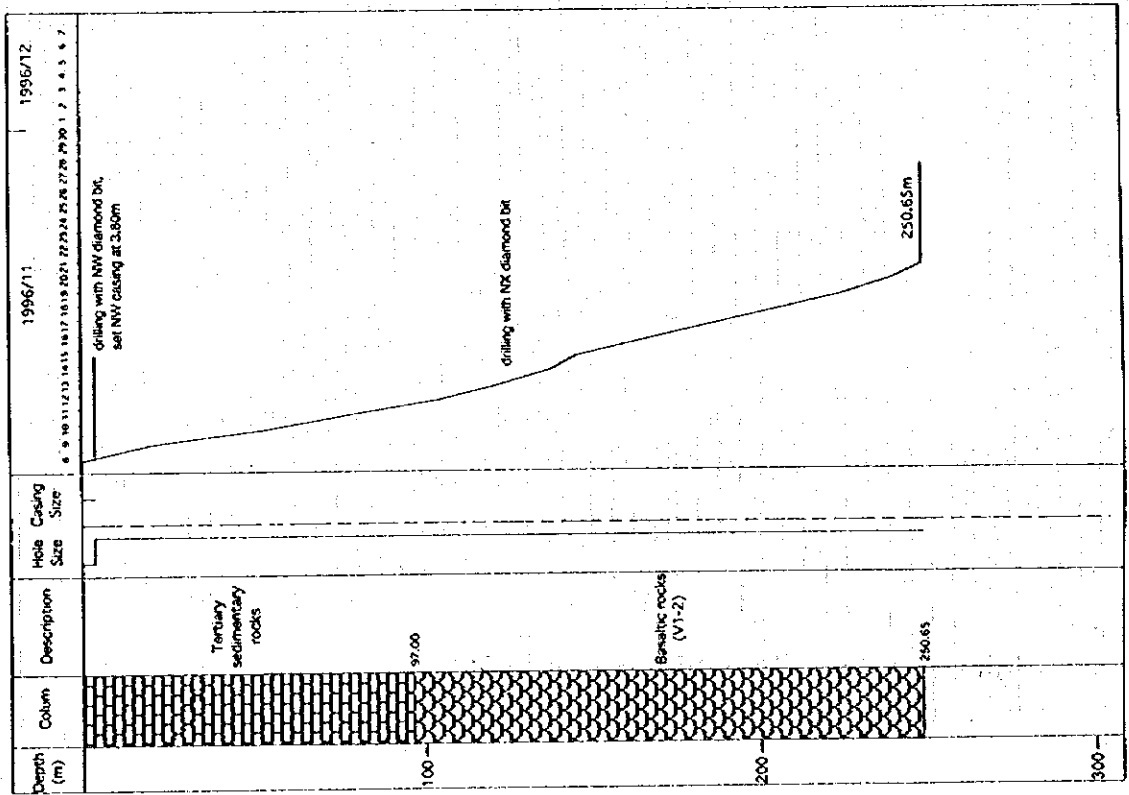
MJOB-A1



MJOB-F2



MJOB-F1



MJOB-R1

